Chemistry Europe
European Chemical Societies Publishing
Batteries & Supercaps

REVIEW OPEN ACCESS

Separator Engineering for Stable Zinc Anodes in Aqueous Zinc-Ion Batteries

Xiao Huang[1,2] | Zhenyu Li[1] | Dongyu Liu[1] | Bowei Wang[1] | Hao Li[3] | Jing Zhang[4] | Hongzhen Lin[2] | Jian Wang[3] | Lei Zhou[1]

[1]School of Energy and Power of Engineering, Jiangsu University, Zhenjiang, China | [2]i-Lab & CAS Key Laboratory of Nanophotonic Materials and Devices, Suzhou Institute of Nano-tech and Nano-bionics, Chinese Academy of Sciences, Suzhou, China | [3]Helmholtz Institute Ulm (HIU), Karlsruhe Institute of Technology (KIT), Karlsruhe, Germany | [4]School of Materials Science and Engineering, Xi'an University of Technology, Xi'an, China

Correspondence: Hongzhen Lin (hzlin2010@sinano.ac.cn) | Jian Wang (wangjian2014@sinano.ac.cn) | Lei Zhou (l.zhou@ujs.edu.cn)

Received: 15 December 2025 | **Revised:** 1 March 2026 | **Accepted:** 4 March 2026

Keywords: hydrogen evolution reaction | separator engineering | zinc anodes | zinc dendrites | zinc-ion batteries

ABSTRACT

Aqueous zinc-ion batteries (ZIBs) have garnered extensive attention due to their advantages of high energy density, low cost, and high safety. However, the practical applications of ZIBs face several crucial challenges, including the uncontrolled growth of zinc dendrites, the parasitic hydrogen evolution reaction, and anode corrosion. These detrimental effects compromise the electrochemical performance of ZIBs, leading to low Coulombic efficiency, short cycle life, and even short-circuit failure. Separator engineering is one of the key approaches to addressing these issues. In this review, we systematically discuss the regulation of zinc anodes through separator engineering. Firstly, we introduce the composition and basic principles of ZIBs. Secondly, effective strategies for regulating zinc anodes through separator engineering are discussed in terms of the modification of commonly used glass fiber (GF) separators and the development of novel separators. Finally, conclusions and an outlook are provided, offering valuable guidance for developing high-performance separator materials of ZIBs. Overall, this review summarizes the current development status of separators, offers perspectives on future development directions, and provides guidance for the advancement of ZIBs.

1 | Introduction

With the rapid consumption of fossil fuels, the exploitation of renewable clean energy has attracted growing attention. Therefore, exploring new technical approaches to develop advanced energy storage systems has become a key focus of contemporary research [1–3]. Lithium-ion batteries(LIBs) possess characteristics, such as high energy density (100-300Wh kg^{-1}), long cycle life, and low self-discharge rate, which have been widely used in electronics, new energy vehicles, and energy storage systems [4–9]. However, lithium-ion batteries currently face challenges, such as approaching the theoretical limit of energy density, resource dependence, high costs, safety risks, and poor adaptability to extreme environments [10]. Developing new battery systems with high safety and cost-effectiveness is the core direction to break through these bottlenecks [11].

Aqueous zinc-ion batteries (ZIBs) are regarded as one of the most promising alternatives for beyond lithium-ion battery systems. Zinc anodes have a high theoretical capacity of about 820 mAh g^{-1} and low electrochemical potential (−0.762V vs. SHE), allowing ZIBs to achieve high energy density [12–14]. Due to their inherent advantages, ZIBs have emerged as promising candidates for next-generation energy storage devices. They feature high safety, low cost, abundant zinc resources, environmental friendliness, and good rate performance. Benefiting from these merits, ZIBs show great potential in large-scale energy storage systems, smart grids, wearable electronics, and low-power portable devices, especially under wide-temperature conditions

[15]. In comparison to LIBs, which currently dominate the consumer electronics and electric vehicle markets, ZIBs offer distinct advantages in terms of safety (being inherently nonflammable), cost (owing to the abundant and inexpensive zinc resources), and environmental friendliness. They are particularly suitable for applications highly sensitive to safety and cost, such as large-scale energy storage, short-distance transportation, and wearable devices. While LIBs target the high-energy-density market, aqueous ZIBs offer a highly attractive solution for building a safer, more sustainable, and lower-cost energy storage future [16–18].

However, ZIBs inevitably face significant challenges during cycling, which severely hinder their practical applications. A critical challenge facing ZIBs is the detrimental growth of zinc dendrites [19, 20]. The essence is that the zinc deposition on the surface of the zinc anode is uneven and forms needle-like crystals, which pierce the separator, consume the electrolyte and negative electrode, and shorten the battery life [21]. Another critical issue is the hydrogen evolution reaction (HER) on zinc anodes. The generation of hydrogen increases the internal pressure of ZIBs, causing battery swelling and hindering ion transport [22, 23]. Moreover, HER reduces the concentration of the electrolyte, which may lead to electrolyte precipitation in severe cases, deteriorating the battery's cycling performance [24]. In addition, the corrosion of zinc anodes in ZIBs refers to the oxidation/dissolution reaction of zinc anodes in the electrolyte, which will seriously affect the stability and cycle-life of ZIBs. It will also lead to the appearance of holes and powdering on the surface of the zinc anode, leading to the collapse of the anode structure [25].

The above-mentioned challenges pose significant obstacles to the development and practical application of ZIBs. Therefore, numerous efforts have been made to tackle these problems from the perspectives of cathode, anodes, separators, and electrolytes, and so on [26–28]. For instance, Fang et al. proposed a kinetic modulation strategy leveraging a spatial electrostatic field layer, which constructed the conjugated system of tetrasulfonated cobalt phthalocyanine ($CoPcS_4$) to boost the preferential Zn (002)-oriented deposition [29]. Both experimental characterizations and theoretical computations verified that $CoPcS_4$ can selectively adsorb onto the electrode surface and form a stable solid electrolyte interphase (SEI), thereby isolating the zinc anode from direct contact with the aqueous electrolyte. The DSFF electrolyte developed by Heo et al.—incorporating dimethyl sulfoxide (DMSO) as the cosolvent and trifluoroethyl formate (FF) as the additive—enabled the formation of a SEI enriched with ZnF_2 and ZnS [30]. This SEI effectively inhibited HER and zinc dendrite growth, endowing the zinc electrode with an ultra-long cycle life of 5500 hr and a CE as high as 99.8%. Both Zn//PANI full cells and pouch cells compatible with this electrolyte demonstrated exceptional cycling stability, rate capability, and energy density under diverse temperature and mass loading conditions. This study offers a novel insight and universal framework for the electrolyte design of high-performance aqueous zinc batteries.

In recent years, research on ZIBs has intensified significantly with respect to electrolytes, Zn anodes, and cathodes, establishing it as a highly active and rapidly evolving field within battery research. Regarding electrolytes, Liu et al. developed a 'polymer-encapsulated water' gel electrolyte with only 20% water content through weak-solvation-monomer-guided polymerization, which maintains a high ionic conductivity of 0.36 mS cm^{-1} even at -70°C [31]. Meanwhile, inspired by food-grade gelatin, Yang et al. designed a thermoreversible sol–gel gelatin-based hydrogel electrolyte that forms a conformal interface on the electrode surface and constructs uniform Zn^{2+} transport channels via SO_4^{2-}-bridged helical gelatin chains [32]. This not only guides uniform zinc deposition but also dynamically repairs interfacial gaps generated during cycling.

In terms of zinc anode protective layers, Guo et al. proposed a high-strength biomimetic interfacial layer inspired by the 'brick-mortar' structure of shells. Combining a high Young's modulus of up to 9.8 GPa with an ionic conductivity of 2.1 mS cm^{-1}, it effectively suppresses zinc dendrite growth and promotes uniform deposition [33]. Zhao et al., inspired by the tolerance mechanisms of extremophyte cell membranes, introduced a tolerance-based interfacial engineering strategy using Pyrostatin B (PyrB) molecules to enhance the cycling stability of zinc anodes under high rates [34]. Through strong electrostatic interactions, a stable molecular layer self-assembles on the zinc anode surface, which not only facilitates Zn^{2+} desolvation and transport and suppresses dendrite growth but also effectively isolates water molecules and reduces side reactions [35].

On the cathode side, Liu et al. proposed the dipeptide molecule aspartame (APM) as an additive to regulate the stripping process of zinc anodes [36]. APM forms an adsorption layer on the zinc surface via its negatively charged centers, increasing the stripping overpotential and promoting uniform zinc dissolution, while its hydrophobic groups repel water molecules and suppress side reactions. Yang et al. proposed a novel cation-screening strategy by intercalating strontium ions (Sr^{2+}) into layered δ-MnO_2 [37]. During charging, partially released Sr^{2+} reacts in situ with sulfate ions in the electrolyte to form an $SrSO_4$ interfacial layer. This interphase combines electronic insulation with ionic conduction, effectively inhibiting manganese dissolution, promoting zinc-ion desolvation, and stabilizing the electrode structure.

Separator engineering is one of the key approaches to addressing these issues facing ZIBs. The separator is a crucial component of ZIBs. Although it does not participate in the reaction, its performance directly affects the battery's service life, performance, safety, and other aspects [38]. In ideal conditions, a separator should exhibit infinitely high electronic resistance and ion resistance approaching zero. The resistivity of polymer separators typically ranges from 10^{12} to 10^{14} Ω cm. However, ion resistivity is affected by the tortuosity of limited porosity and open porous structures, which elongates the average path of ion current. Therefore, designing separators with high porosity and uniform pore diameters while ensuring mechanical strength has become a critical research direction [39].

Among them, glass fiber (GF) separators are widely used in ZIBs due to their excellent hydrophilicity, porosity, and ion transport capability [40, 41]. However, the poor ionic conductivity of GF affects the reaction rate and reversibility of ZIBs [42]. Additionally, the large pores of GF lead to uneven deposition of zinc ions, causing the formation of zinc dendrites. Moreover, the insufficient mechanical properties of GF separators allow zinc dendrites to pierce through the separator, posing hazards to the battery [43]. In addition, some novel separators have been used in ZIBs, such as cellulose separators, which

exhibit high mechanical strength, excellent hydrophilicity, and good insulating properties [44–46].

Previous reviews primarily focus on material summaries. For instance, Li et al. introduced two optimization strategies: one involves material modifications to commonly used GF separators, and the other focuses on developing novel separators [47]. Zong et al. analyzed the key roles of functionalized separators in homogenizing zinc ion transport, suppressing dendrite growth, preventing cathode dissolution, and blocking shuttling dissolved ions, providing a detailed introduction to various preparation techniques [48]. Additionally, Li et al. reviewed improvement strategies for zinc-ion battery separators, analyzed their key performance requirements, and discussed in detail optimization methods and their impact on battery performance for different types of separators such as GF, cellulose, and polymers [49]. In contrast, this review breaks through the traditional perception of separators merely as physical barriers and focuses on "separator engineering" for actively regulating performance of Zn anodes. We systematically categorize separator strategies for stable zinc anodes into two main pathways: surface functionalization of commercial GF separators and the development of novel separators such as cellulose-based, biomass-derived, and Janus-structured materials. Furthermore, this review delves into the mechanisms by which these materials stabilize zinc anodes—by regulating ion transport, guiding uniform deposition, and suppressing side reactions. Finally, we propose practical and promising research directions for separator engineering, which provide useful insights into developing high-performance and stable ZIBs.

In this review, we systematically summarize the latest advances of separator engineering for addressing the critical challenges facing zinc anodes in ZIBs. Firstly, the configurations and reaction principles of ZIBs are presented. Then, we summarize strategies for regulating zinc anodes through separator engineering, which is divided into two aspects: modification of commonly used GF separators and development of novel separators (Figure 1). Based on material types and modification methods, their enhancement effects on zinc anodes are analyzed. The mechanisms of separator engineering on the uniform migration and deposition of Zn^{2+}, suppressing dendrite growth, and inhibiting side reactions are discussed. Finally, conclusions and an outlook are provided, offering valuable guidance for developing high-performance separator materials of ZIBs.

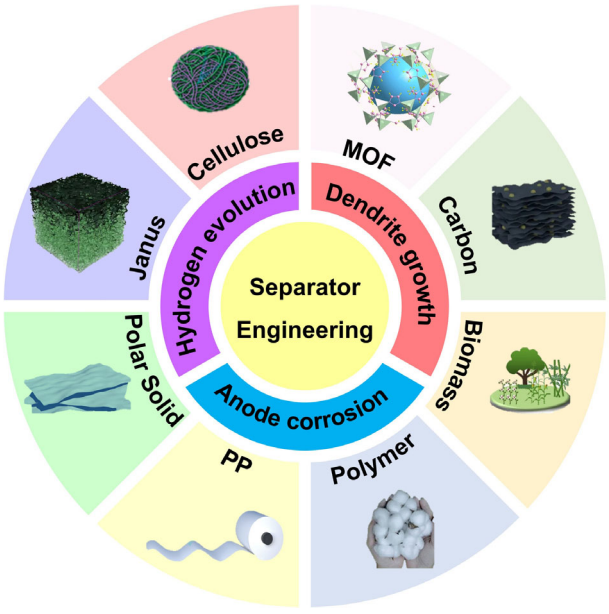

FIGURE 1 | Schematic diagram of separator engineering for ZIBs.

2 | Reaction Principle and Interaction Mechanism

2.1 | Basic Principles

Figure 2 presents the basic configurations of ZIBs. Typically, ZIBs employ metallic zinc as the anode, a zinc-ion-rich aqueous solution (such as $ZnSO_4$) as the electrolyte, and materials capable of reversibly hosting zinc ions (such as manganese dioxide or vanadium-based oxides) as the cathode [50]. The essence of the charging and discharging of ZIBs lies in the reversible intercalation/deintercalation of Zn^{2+} between the cathode and anode. During discharging, the zinc anode undergoes oxidative dissolution, and Zn^{2+} migrates to the cathode and intercalates into the host materials. During charging, the reaction proceeds in the reverse direction, where Zn^{2+} deintercalates from the cathode and is reduced to metallic zinc through deposition on the anode [51].

Numerous types of cathode materials have been developed in ZIBs. Taking the most typical manganese dioxide (MnO_2) cathode as an example, the underlying reaction mechanism of the MnO_2 cathode in Zn-MnO_2 batteries remains intricate, which can be concisely summarized as [52]

$$\text{Anode: } Zn - 2e^- \leftrightarrow Zn^{2+} \tag{1}$$

$$\text{Cathode: } Zn^{2+} + 2e^- + 2MnO_2 \leftrightarrow ZnMn_2O_4 \tag{2}$$

$$\text{Full battery reaction: } Zn + MnO_2 \leftrightarrow ZnMn_2O_4 \tag{3}$$

During battery cycling, a series of parasitic reactions occur, such as HER, which spoil the zinc anode. HER alters the internal pressure of ZIBs, which in turn causes electrolyte leakage and consumption, ultimately leading to severe safety hazards. This issue is particularly prominent in sealed battery systems. During the progression of HER, the consumption of H^+ results in an increased concentration of OH^- in the region adjacent to the anode surface. Subsequently, metallic zinc reacts with OH^- ions to form $Zn(OH)_4^{2-}$. When $Zn(OH)_4^{2-}$ reaches a supersaturated state, it precipitates and transforms into $Zn(OH)_2$. The generated $Zn(OH)_2$ then undergoes a dehydration reaction, eventually forming solid ZnO. The aforementioned reaction processes are described in Equations (4) – (6), while the reaction corresponding to the scenario where $ZnSO_4$ is present in the electrolyte is specified in Equation (7).

$$Zn(s) + 4OH^- \leftrightarrow Zn(OH)_4^{2-} + 2e^- \tag{4}$$

$$Zn(OH)_4^{2-} \leftrightarrow Zn(OH)_2(s) + 2OH^- \tag{5}$$

$$Zn(OH)_2(s) \leftrightarrow ZnO \cdot (s) + H_2O \tag{6}$$

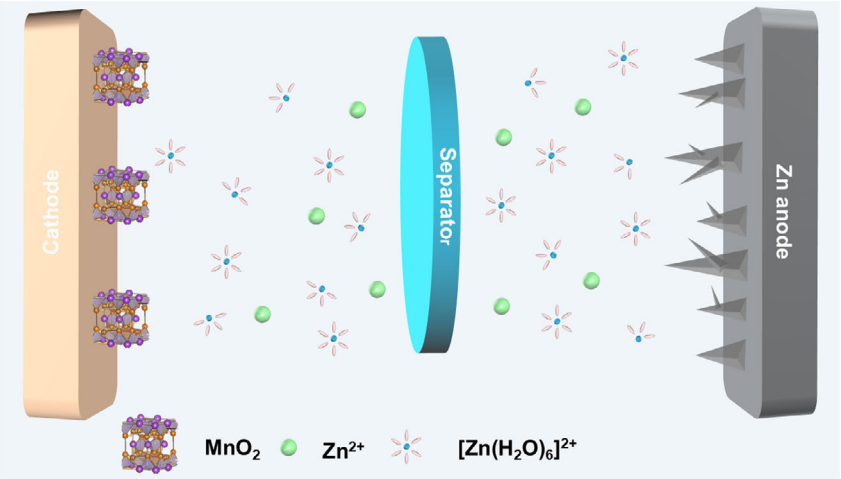

FIGURE 2 | Schematic diagram of basic configurations of ZIBs.

$$4Zn^{2+} + SO_4{}^{2-} + 6OH^- + nH_2O \leftrightarrow Zn_4SO_4(OH)_6 \cdot nH_2O \quad (7)$$

This series of reactions involves multiple interfacial transformation and mass transfer processes, and the core issues that may arise include: local electrolyte pH fluctuations caused by the mismatch between the consumption and regeneration rates of OH^- ions during the reaction, increased mass transfer resistance induced by the uneven deposition and agglomeration of $Zn(OH)_2$/ZnO products on the electrode surface, and intensified reaction polarization resulting from the kinetic differences among the multistep transformation reactions. All these issues may affect the cycle stability, rate performance, and energy efficiency of the battery [53].

2.2 | Interaction Mechanism

The molecular–level interaction mechanism at the functional groups on the separator surface fundamentally relies on precisely designed coordination or electrostatic interactions between chemical groups and Zn^{2+} to regulate the solvation structure and transport behavior of zinc ions at the interface. For instance, electron-rich functional groups such as carbonyl groups can partially replace water molecules in the original hydration shell of Zn^{2+}, weakening the solvation effect and reducing the desolvation energy barrier. Simultaneously, these functional groups form dynamic ion adsorption/release sites on the separator surface, which homogenize the interfacial electric field distribution and guide Zn^{2+} to preferentially nucleate and undergo epitaxial growth along low-energy crystal planes, such as the (002) plane. This molecular-level interfacial engineering not only accelerates ion transport kinetics but, more importantly, fundamentally suppresses the random growth of dendrites by inducing uniform ion flux and nucleation site distribution. As a result, it achieves significant improvements in the controllability of zinc deposition morphology and cycling stability [54].

In addition, physical loading is also a core mechanism for regulating zinc-ion deposition behavior. Its essence lies in introducing nanomaterials with specific physical structures and surface properties to directly alter the microscopic morphology and interfacial characteristics of the separator. These materials do not rely on chemical bonding; instead, they leverage their lattice-matching relationship with zinc metal, abundant surface functional groups, and unique two-dimensional layered structure to construct ordered ion transport channels and nucleation guidance sites on the separator surface. For example, graphene oxide (GO) not only absorbs and uniformly distributes Zn^{2+} through its surface oxygen-containing functional groups but also utilizes its small lattice mismatch with the zinc (002) crystal plane to induce epitaxial deposition of Zn^{2+}. This physically constrains the deposition direction and suppresses the vertical growth of dendrites, ultimately significantly enhancing the cycling stability and deposition reversibility of the battery under high current densities [55].

The foregoing discussion outlines the basic configuration and charge–discharge reaction mechanism of ZIBs, clarifying that the intercalation/deintercalation of Zn^{2+} between the cathode and anode constitutes the core process of battery charging and discharging. Meanwhile, it reveals the molecular–level interaction mechanism of functional groups on the separator surface, specifically the regulation of the solvation structure and transport behavior of zinc ions through coordination or electrostatic interactions, as well as the approach of constructing ordered ion transport channels via physical loading of nanomaterials. These two aspects work synergistically to achieve uniform Zn^{2+} deposition, suppress dendrite growth and side reactions, and thus enhance the cycling stability of ZIBs.

3 | Critical Challenges Facing Stable Zn Anodes

3.1 | Uncontrolled Growth of Zinc Dendrites

ZIBs encounter various difficulties and challenges during cycling (Figure 3), which is similar to Li ion/metal batteries [56–60]. The growth of zinc dendrites in ZIBs leads to uneven deposition on the zinc anode, separator piercing, and eventually battery failure [61]. As a core component of the battery, the separator can inhibit dendrite growth through multidimensional regulation: optimizing the pore structure of separators (e.g., constructing uniform microporous channels suitable for zinc ion transport), introducing zinc-philic functional groups (such as hydroxyl and amino groups) or ion-selective functional groups (such as sulfonic acid and carboxyl groups) to improve zinc ion adsorption and uniform

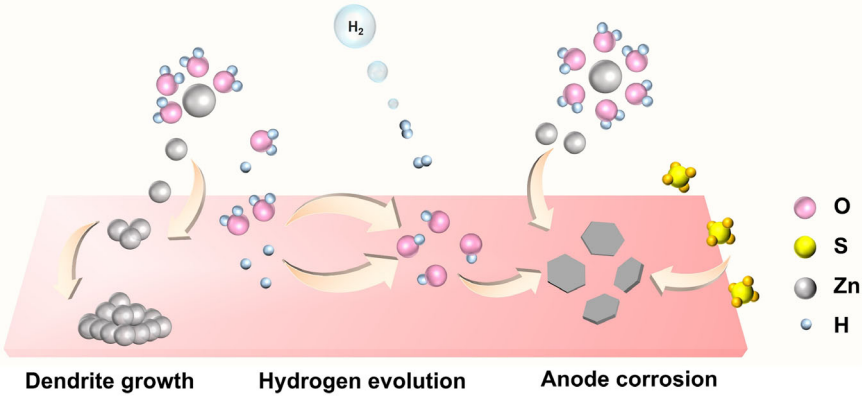

FIGURE 3 | Schematic diagram of challenges facing stable Zn anodes.

distribution, thereby reducing local ion concentration gradients; adopting composite modification strategies (e.g., compounding conductive nanoparticles, inorganic ceramic fillers, or polymer coatings) to enhance the mechanical strength and interfacial compatibility of separators, thus suppressing dendrite piercing; designing functional separators to regulate zinc ion transport kinetics and guide uniform zinc ion deposition. These approaches synergistically inhibit zinc dendrite growth and improve the long-term cycle stability of batteries [62].

3.2 | HER on Zn anodes

HER on Zn anodes leads to electrolyte consumption, decreased battery CE, and potential safety hazards [63]. As a key regulatory carrier, the separator can inhibit HER through multifunctional design: introducing proton-selective barrier functional groups, such as quaternary ammonium salts and -SO_3H or constructing densified interfacial layers to reduce the adsorption and transport efficiency of hydrogen ions on the electrode surface [64], thereby weakening the thermodynamic driving force of HER; adopting hydrophilic/ion-conductive composite modification (e.g., compounding metal-organic frameworks (MOFs), ceramic nanoparticles, or ion-exchange resins) to optimize electrolyte wettability and zinc ion transference number, alleviating local hydrogen ion enrichment; designing separators with electrocatalytic inhibition functions, such as loading HER-inert catalysts or modifying conductive components to increase the HER reaction energy barrier, accelerate uniform zinc ion deposition, and enhance the mechanical stability of the separator to avoid aggravated HER caused by interfacial damage. These strategies synergistically suppress the hydrogen evolution side reaction and ensure the electrochemical performance of the battery [65].

3.3 | Anode corrosion

Anode corrosion in ZIBs causes loss of zinc electrode materials, electrolyte deterioration, and shortened cycle life,[28, 66–68] which can be synergistically inhibited by the targeted design of separators: introducing corrosion-inhibiting functional groups to form a protective adsorption layer on the zinc electrode surface; performing zinc-philic/ion-selective composite modification to reduce the enrichment of corrosive media on the anode surface; and adopting barrier-type functional separators to physically isolate corrosive factors while optimizing interfacial stability, thereby ensuring the long-term electrochemical performance of the battery [69].

In summary, the three primary challenges that restrict the stable cycling of zinc anodes, namely the uncontrolled growth of zinc dendrites, the hydrogen evolution side reaction, and anode corrosion. Zinc dendrites can pierce the separator and cause internal short circuits of the battery; HER consumes the electrolyte and leads to battery swelling, thus reducing the Coulombic efficiency (CE); anode corrosion results in structural pulverization and failure of the zinc electrode. Separator engineering can address problems in a targeted manner through approaches such as pore structure optimization, introduction of functional groups and composite modification, which act by regulating ion transport and enhancing mechanical strength.

4 | Separator Engineering for Improving Zn Anodes

Traditional ZIB separators (such as GF separators) primarily serve the simple function of physically isolating the positive and negative electrodes to prevent short circuits [70]. In contrast, separator engineering is a key approach to regulating the performance of ZIBs, which involves the design and modification of separators through physical and chemical methods, enabling them to actively regulate zinc deposition behavior, inhibit zinc dendrite growth, suppress side reactions, and enhance the overall battery performance. The mechanism achieves precise regulation of ion migration and electrode interface reactions through separator structural design, interface modification, and functionalization. Designing separators with confinement effects can prevent the growth of zinc dendrites, avoiding battery short-circuit failure. By regulating the pore size, porosity, and hydrophilic-hydrophobic properties of the separator, the Zn^{2+} ion conductivity can be improved, thus enhancing the reaction kinetics. Furthermore, separator engineering can block excessive contact between electrodes and electrolytes, reducing side reactions, zinc anode passivation, and cathode dissolution, thereby improving battery CE and cycle stability [71]. The specific strategies for separator engineering mainly include: (1) surface modification of separators (e.g., coating nanomaterials or MOFs) to optimize the wettability and chemical interactions at the electrode-separator

interface, guide uniform Zn^{2+} deposition, and reduce interface side reactions and impedance and (2) developing novel separator structures to construct ordered pore structures, enhance electrolyte wettability, and regulate zinc ion flux for uniform deposition [72].

4.1 | Surface modification of GF separators

GF separators are one of the most commonly used separators in ZIBs due to their high porosity, favorable hydrophilicity, excellent chemical stability, and low cost [68, 73]. However, they also possess several defects, which limit cycling stability and the safety of ZIBs. The most critical drawback of GF separators is the poor mechanical strength. GF separators with less flexibility are inherently brittle and prone to tearing or pulverization under pressure during battery assembly or cycling. More importantly, their low puncture resistance fails to effectively block the growth of zinc dendrites, rendering internal short circuits in batteries. In addition, the ionic conductivity of GF separators is lower than that of polymer composite separators, resulting in a low Zn^{2+} transference number. Furthermore, the pore structure of GF separators is disordered, and the size distribution is wide (mostly micron-scale), thus failing to effectively guide uniform zinc ion flux. This exacerbates uneven Zn^{2+} deposition and promotes zinc dendrite growth. Therefore, rational surface modification of GF separators can significantly overcome these issues [74].

4.1.1 | MOF modified GF separators

In situ modification of MOFs on GF separators is able to effectively regulate the distribution of zinc ions through zinc affinity, thereby effectively inhibiting the growth of dendrites [75–77]. Zeolitic imidazolate framework (ZIF) as functional modification materials for ZIBs possess regular, ordered, size-tunable nanochannels and strong chemical stability. These advantages allow them to guide uniform deposition of Zn^{2+}, improve ion sieving, and block excessive contact between electrodes and electrolytes, which effectively inhibit zinc dendrites, optimize ion transport, and suppress side reactions. For instance, ZIF-8 has been coated on the GF separator to improve the performance of ZIBs. The insulating property of ZIF-8 can reduce HER, the hydrophobicity can prevent the occurrence of side reactions, and the ordered nanochannels can promote the uniform deposition of Zn^{2+} [78, 79]. Zhang et al. in situ synthesized ZIF-8 on GF via a hydrothermal method [80]. The high nitrogen content of ZIF-8 effectively regulated $[Zn(H_2O)_6]^{2+}$ to reduce hydrogen production. Its abundant nanochannels enabled localized effects that promoted uniform Zn^{2+} deposition, thereby inhibiting dendrite formation. Moreover, scanning electron microscopy (SEM) images reveal that the synthesized ZIF-8-GF is denser, which promotes more uniform deposition of Zn^{2+} (Figure 4a,b). Furthermore, ZIF-8 contains elements such as C, O, and Zn (Figure 4c). At 1.2 A g^{-1}, the Zn//MnO_2 battery assembled with ZIF-8-GF exhibited higher capacity retention and discharge capacity, which confirmed its better cycle performance.

Beyond ZIF-8, other ZIF variants have been investigated for separator modification in ZIBs. Hao et al. coated a three-dimensional hexapod fluorinated zeolite imidazolium framework (H-F-ZIF) scaffold onto GF and applied it in ZIBs [81]. The strong electrostatic interaction between fluorine functional groups (-CF_3) and I_3^- effectively anchored polyiodides. SEM observation in Figure 4d reveals an orthogonal structure of the H-F-ZIF, while high-magnification SEM shows a more detailed morphology: a cross-shaped prism (Figure 4e). This structure significantly increased the specific surface area in contact with the electrolyte. Additionally, the elemental distribution of C, Zn, N, and F was highly uniform, confirming successful fluorine incorporation (Figure 4f). Density functional theory (DFT) calculations were performed to investigate the adsorption properties of I_3^- on H-F-ZIF and ZIF-8. First, the binding free energy of I_3^- with the Zn^{2+}-imidazole (Melm) unit in ZIF-8 was −0.47 eV, while that of I_3^- with the Zn^{2+}-imidazole-trifluoroacetate (Melm-TFA) unit in H-F-ZIF was −0.64 eV. This result indicated that the -CF_3 group can enhance the adsorption of I_3^-(Figure 4g). The adsorption energy of I_3^- on ZIF-8 was −0.56 eV, and that on H-F-ZIF was −0.95 eV, confirming that the electron-withdrawing -CF_3 group can effectively strengthen the adsorption capacity for I_3^-(Figure 4h).

UiO-66, a Zr-based MOF, when modified on separators, can effectively enhance carrier transport capacity, exhibit corrosion resistance, and suppress dendrite formation [82]. The large specific surface area can promote redox kinetics. Additionally, UiO-66 exhibits more stable chemical properties in weakly acidic electrolytes [83]. For example, Song et al. developed high-performance ZIBs by modifying UiO-66 on the GF separator, resulting in the UiO-66-GF composite material [84]. UiO-66-GF promoted zinc ion growth on the (002) plane, ultimately forming dendrite-free zinc deposits (Figure 5a-b). Results show that at 2.0 mA cm^{-2}, the Zn|UiO-66-GF-2.2|Zn symmetric cell exhibited good plating/stripping reversibility and a cycle life over 1650 h. The Zn|UiO-66-GF-2.2|MnO_2 full cell achieved 85% capacity retention after 1000 cycles with excellent long-term stability. Rational design and application of multifunctional MOF-modified separators offer valuable guidance for high-performance and long-cycle-life ZIBs.

In addition to pristine UiO-66, sulfonated derivatives such as UiO-S2 have demonstrated enhanced functionality in separator modification. Chen et al. developed a novel stabilization strategy for zinc anodes in ZIBs by modifying GF separators with -SO_3H functionalized UiO-66 [85]. Bis-sulfonate UiO-66 (UiO-S2) was prepared via the postsynthetic oxidation of dithiol-functionalized UiO-66 (denoted as UiO-SH). Specifically, the reaction between 2,5-dimercapto-1,4-benzenedicarboxylic acid and $ZrCl_4$ resulted in the precipitation of UiO-SH. For comparison, UiO-S1 and UiO-66 were synthesized by a one-step solvothermal method (Figure 5c). The sulfonate-functionalized UiO-66 GF separator (GF@UiO-S2) leveraged strong zinc-affinity interactions between -SO_3H groups and Zn^{2+} ions, achieving both uniform ion flux distribution and accelerated ion migration kinetics. During Zn^{2+} deposition, -SO_3H provided effective protection for the zinc anode, while bis-sulfonic acid groups demonstrated superior affinity for promoting rapid desolvation of zinc, thereby reducing corrosion (Figure 5d).

4.1.2 | Polymer Modified GF Separators

Polymers can effectively optimize ion transport, suppress dendrite growth and side reactions, and enhance the mechanical properties of batteries [86–89]. Commonly used polymers include polyimide (PI), polyacrylonitrile (PAN), and polyvinylidene

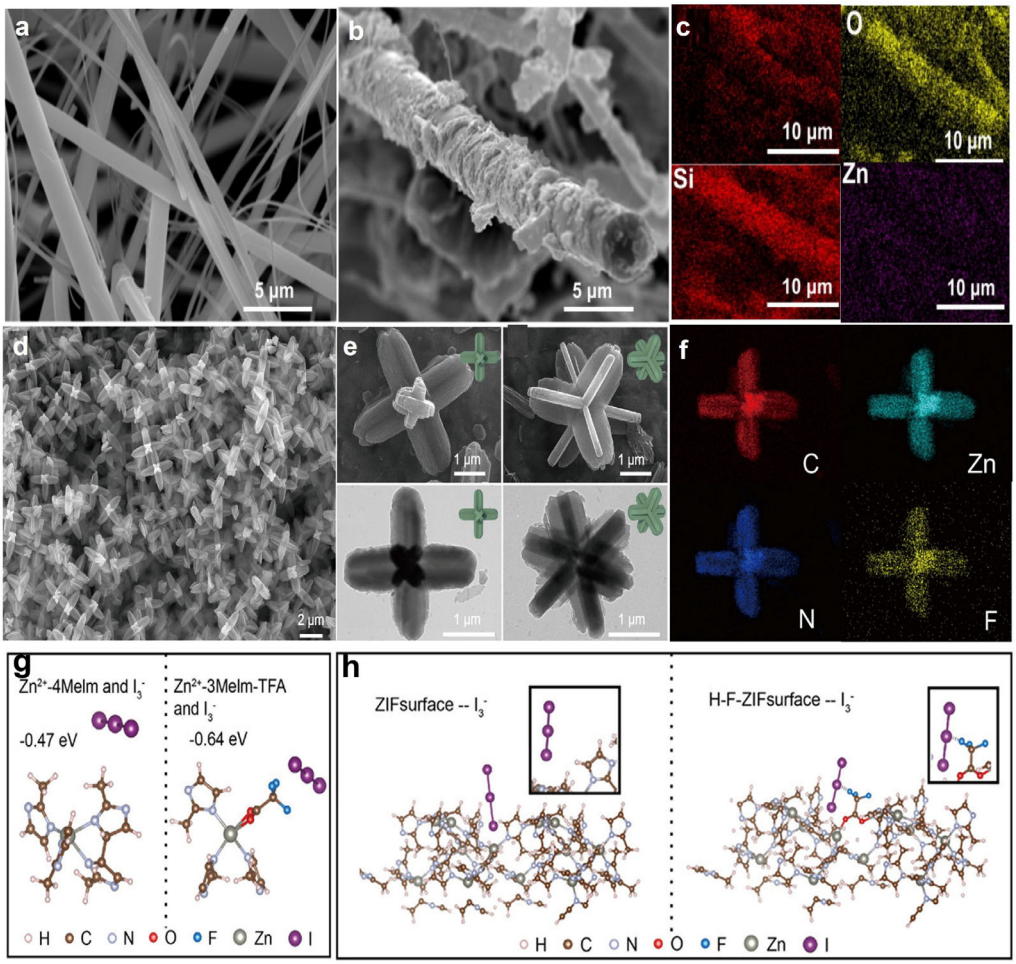

FIGURE 4 | (a) SEM image of GF [80]. (b and c) SEM image of ZIF-8-GF and element mapping for C, O, Al, and Zn. Reproduced with permission [80]. Copyright 2024, Elsevier. (d) FESEM image of H-F-ZIF [81]. (e) FESEM and TEM images of H-F-ZIF particles in different orientations with the insets showing the schematic models [81]. (f) Elemental mapping images of H-F-ZIF [81]. (g) Calculation models of the interaction between the I_3^- ion and Zn^{2+}-4Melm unit (left), and the I_3^- ion and Zn^{2+}-3Melm-TFA unit (right) [81]. (h) DFT calculated absorption models of I_3^- on the surface of ZIF and H-F-ZIF. Reproduced with permission [81]. Copyright 2025, Wiley-VCH.

fluoride (PVDF). These polymers possess excellent properties. For example, the carbonyl groups in the imide groups (–CO–N–CO–) of PI can effectively adsorb Zn^{2+}, facilitating the rapid transport of Zn^{2+}, reducing the nucleation overpotential, and accelerating the redox kinetics. In addition, the -CN bonds in PAN can promote uniform distribution of the electric field, enabling uniform deposition of Zn^{2+} and avoiding the formation of zinc dendrites. PVDF has high mechanical strength and excellent electrochemical stability. However, the high crystallinity of PVDF separators leads to poor ionic conductivity. Therefore, the modification of PVDF with functional groups or coordination bonds to improve ionic conductivity has become a research focus [90].

In ZIBs, PI-modified GF offers key advantages via structural compounding and performance complementarity: enhanced mechanical stability/anti-dendrite penetration, optimized electrolyte wettability/ion transport, improved acid resistance/chemical stability, and promoted uniform zinc deposition. They balance mechanical support, ion transport, and interfacial stability, boosting battery rate performance, cycle life, and safety. Farva et al. developed a PI-functionalized GF separator (PI-GF) via a simplified dip-coating method [91]. The imide groups (-CO-N-CO-) in PI molecules exhibited strong zinc adsorption via the carbonyl groups, which enhanced Zn^{2+} conduction, reduced nucleation overpotential, and enabled rapid reaction kinetics. This composite separator effectively mitigated concentration polarization promoted uniform Zn^{2+} deposition to suppress dendrite growth, and consequently significantly improved the stability of zinc anodes. The results show that at 0.5mA cm^{-2}, the composite separator can ensure the battery stably cycles for 4000 h with stable cycling performance (Figure 6a). Under the flame, the GF separator shrinks and deforms, while the composite separator only has a little carbonization, confirming that the PI composite separator has high thermal stability (Figure 6b,c). Furthermore, the highest occupied molecular orbital/lowest unoccupied molecular orbital (HOMO/LUMO) energy level diagram reveals that the PI molecule exhibits a narrow HOMO-LUMO gap, which enhances the polymer monomer's electrical conductivity. This characteristic indicates that the modified PI demonstrates superior electron transfer capability compared to conventional PI (Figure 6d).

To further verify the universality of the modification effect of PI on GF separators and optimize the preparation process for broader applicability. Liu et al. fabricated a PI-functionalized

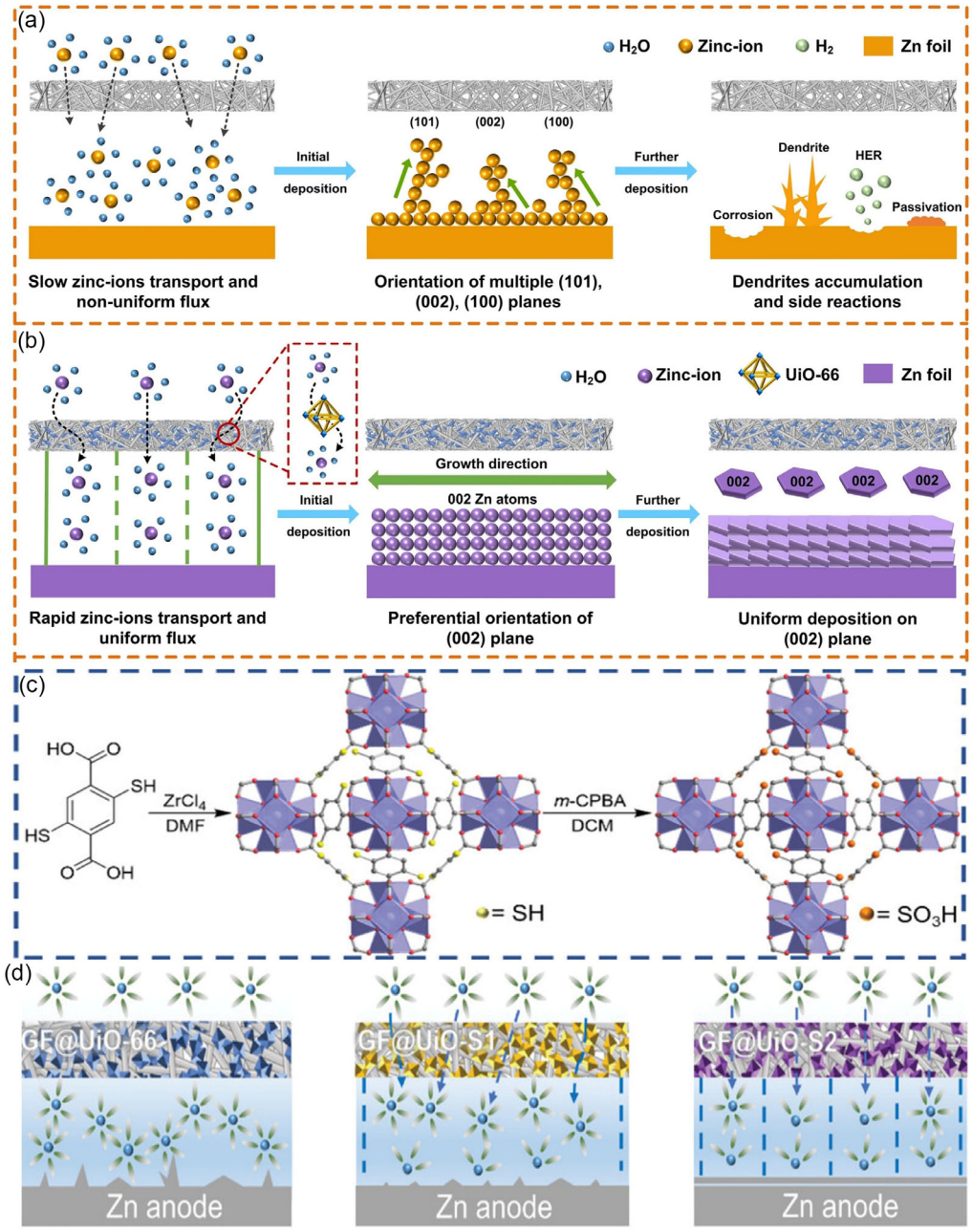

FIGURE 5 | (a) GF and (b) UiO-66-GF-2.2. Reproduced with permission [84]. Copyright 2022, Springer Nature. (c) Illustration of the synthesis of UiO-S2 [85]. (d) GF@UiO-66, GF@UiO-S1, and GF@UiO-S2 separators. Reproduced with permission [85]. Copyright 2025, Elsevier.

GF separator (PI-GF) via a simple drop-coating method [92]. Leveraging the strong adsorption of carbonyl groups in PI's imide moieties (-CO-N-CO-) toward zinc (Zn), they optimized Zn^{2+} conduction efficiency, reduced nucleation overpotential, and achieved rapid reaction kinetics. For the Cu//Zn battery system, the cells equipped with the PI-GF separator exhibited excellent overlap of charge–discharge voltage profiles at the 100th, 500th, and even 1700 cycles, fully demonstrating outstanding electrochemical reversibility (Figure 6e). Additionally, rate performance tests of full cells with V_2O_5 as the cathode and Zn as the anode revealed that PI-GF delivered a higher discharge capacity of 235.5 mAh g^{-1} (Figure 6f). This composite separator effectively mitigates concentration polarization, suppresses dendrite growth, and significantly enhances the operational stability of zinc anodes (Figure 6g).

The porous structure of PAN can effectively regulate uneven zinc ion deposition, and their rich nitrogen-containing groups can fully absorb water to inhibit the occurrence of HER. Li et al. mixed PAN and zinc bis(trifluoromethanesulfonyl) imide (ZnTFSI) in a certain ratio in N, N-dimethylformamide (DMF), and then in situ synthesized the mixture on GF via electrospinning to prepare the PAN-ZnTFSI (PZ) fibrous separator (Figure 7a) [93]. The denser pores of PZ enabled better deposition of Zn^{2+}. Meanwhile, the electrospinning process caused the rearrangement and recombination of electric dipoles, endowing PZ with lower crystallinity. The reduced crystalline further gave PZ higher mechanical properties and a more uniform surface compared with GF. Moreover, PZ possessed excellent wettability, which facilitated the desolvation process and thereby reduced the occurrence of side reactions. The results show that even at

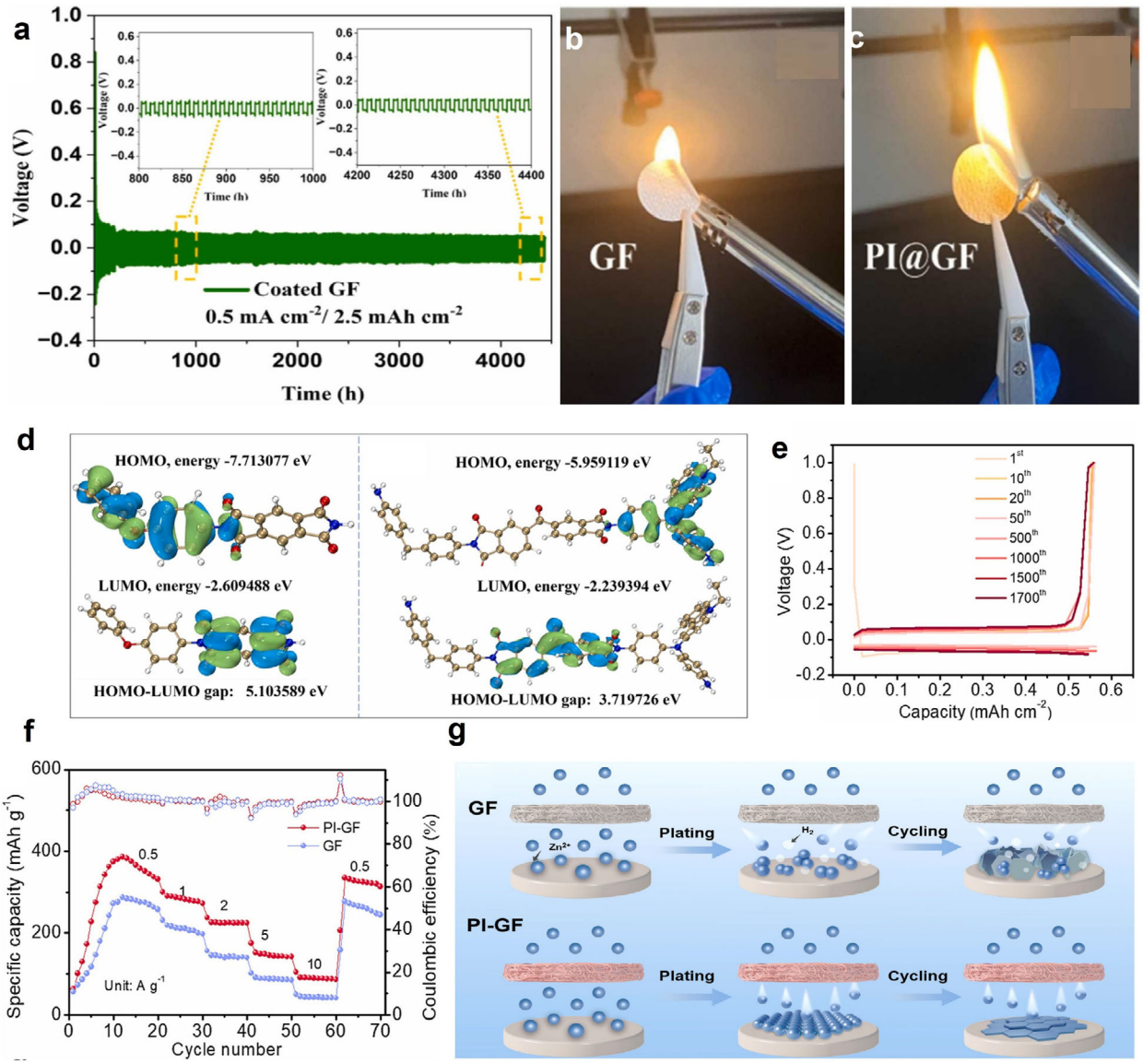

FIGURE 6 | (a) Voltage profiles of Zn//Zn symmetric cells with PI@GF at 0.5 mA cm^{-2}/2.5 mAh cm^{-2} [91]; Flammability tests on (b) bare-GF (c) PI@GF [91]; (d) HOMO/LUMO energy level diagrams of this work PI and normal PI molecules; Reproduced with permission [91]. Copyright 2024, Elsevier. (e) Voltage profiles of the Zn//Cu battery with the PI-GF separator [92]. (f) Rate performances of full batteries based on GF and PI-GF separators [92]; (g) Schematic illustration for the Zn deposition mechanism with GF and PI-GF separators. Reproduced with permission [92]. Copyright 2024, Elsevier.

0.5A g^{-1}, the Zn//VO_2 full cell assembled with the PZ-GF composite film exhibited exceptional long-cycle stability, achieving 1200 cycles with a capacity retention rate of 75%.

Building upon the modification effect of PAN-based composite separators on regulating Zn^{2+} deposition, a more elaborate design of PAN separators was subsequently proposed. Fang et al. designed a 3D long-range ordered PAN nanofiber separator [94]. The N atoms on the surface of this separator can achieve uniform distribution of ion flux and guide cation transport through the formation of N-Zn coordination bonds, thereby homogenizing the electric field distribution on the anode surface and providing ordered guidance for the nucleation, growth, and deposition of Zn^{2+}. Benefiting from this functional group regulation effect, the Zn symmetric cell equipped with the PAN separator not only exhibited excellent long-term cycling stability but also obtained a dendrite-free Zn deposition layer with a preferred (101) crystallographic orientation. In addition, the electric field distribution of the GF separator is nonuniform (Figure 7b,c), whereas the electrostatic interaction between PAN and Zn^{2+} enables uniform electric field distribution, which promotes the uniform deposition of Zn^{2+} (Figure 7d,e).

PVDF modification of ZIBs separators can enhance the mechanical properties of separators and inhibit the occurrence of side reactions, but it suffers from poor ionic conductivity and strong hydrophobicity. Wu et al. modified GF with a dispersion of graphite fluoride nanosheets (GFN) and PVDF via vacuum filtration, successfully fabricating the GFNs-PVDF@GF composite separator [95]. This modification strategy not only enhances the ionic conductivity of the separator but also effectively suppresses the occurrence of side reactions. Meanwhile, the

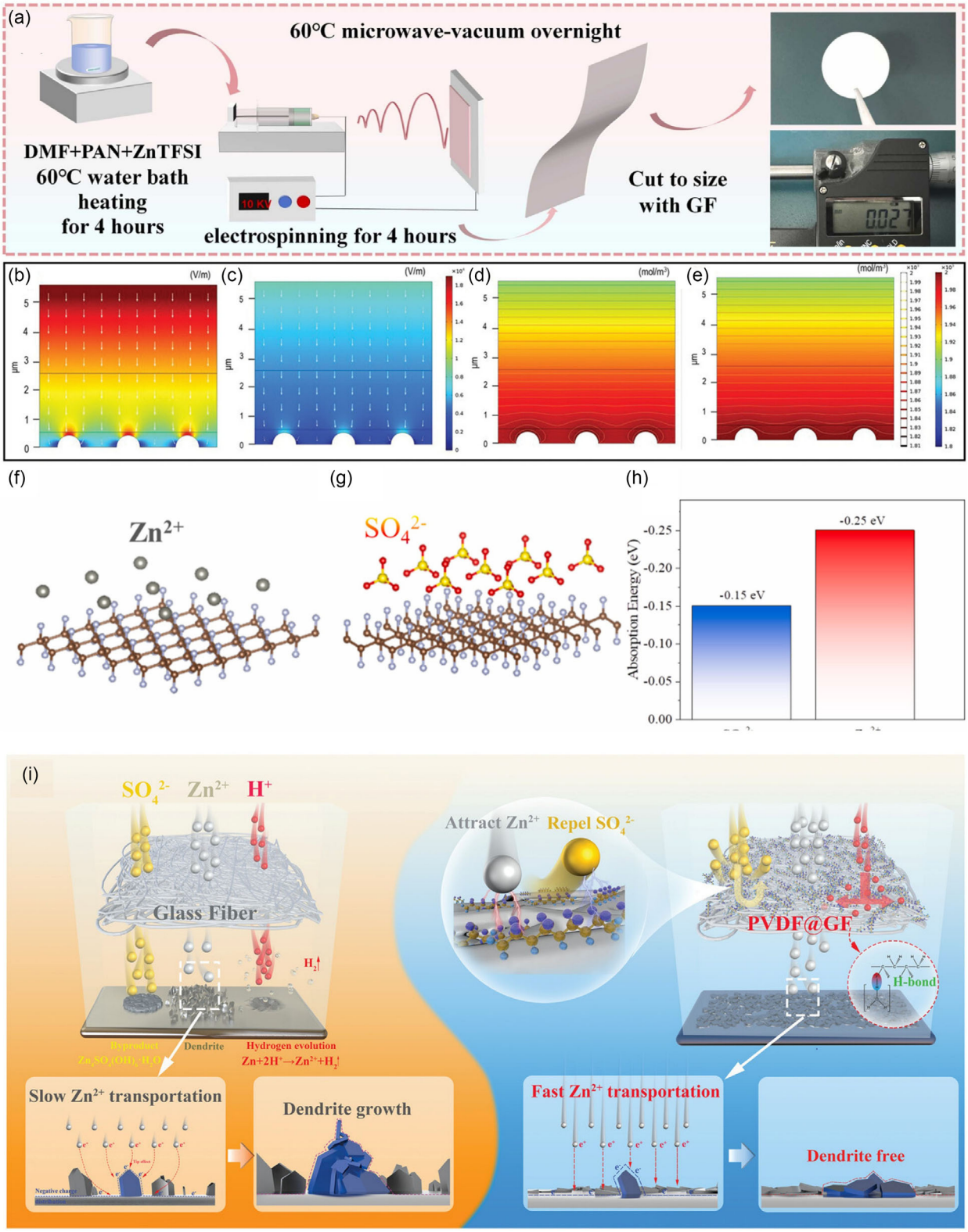

FIGURE 7 | (a) Manufacturing process for PZ separators; Reproduced with permission [93]. Copyright 2024, Elsevier. Electrical field models based on (b) the GF separator and (c) PAN separator [94]. Zinc ion concentration field models based on (d) the GF separator and (e) PAN separator. Reproduced with permission [94]. Copyright 2021, Wiley-VCH. (f,g) The structure model of Zn^{2+} and SO_4^{2-} around adsorbed fluorine sites by the side of the GFNs, respectively [95]. (h) Binding energies of fluorine element and different ion species through DFT calculations. Reproduced with permission [95]. Copyright 2023, Elsevier. (i) Mechanism diagram of PVDF@GF separator-mediated triple ions (Zn^{2+}, SO_4^{2-}, and H^+) behavior to simultaneously resolve Zn anode issues. Reproduced with permission [96]. Copyright 2023, Wiley-VCH.

composite separator significantly reduced zinc dendrite formation by blocking the migration flux of SO_4^{2-}. Benefiting from its lower charge transfer resistance, the GFNs-PVDF@GF composite separator exhibited superior redox kinetics. In addition, GFN possessed strong zinc philicity and high electronegativity, a feature that inhibited the passivation of the zinc anode while improving the reversibility of its deposition/dissolution processes. In the model structure, Zn^{2+} and SO_4^{2-} are attracted by fluorine atoms (Figure 7f,g), and the higher binding energy between fluorine and Zn^{2+} confirms its preferential adsorption toward Zn^{2+}(Figure 7h), accelerating the desolvation of Zn^{2+}. Results show that the Zn//MnO_2 full cell assembled with this composite separator retained 92% of its initial capacity after 200 cycles at a current density of 1 A g^{-1}.

In addition to the composite modification strategy combining PVDF with GFN, grafting modification of PVDF on GF separators has also been explored. Shen et al. modified the surface of GF with PVDF via a grafting method, successfully fabricating the PVDF@GF composite separator [96]. This modification strategy can effectively achieve the uniform redistribution of Zn^{2+}, enhance the transport efficiency of Zn^{2+}, and suppress the occurrence of side reactions. After cycling tests, a large amount of aggregated "dead zinc" and numerous by-products appeared on the surface of the pristine GF separator, leading to the irreversible loss of Zn^{2+}. In contrast, the PVDF@GF composite separator still maintained a relatively smooth surface morphology, its original porous structure was well preserved, and the reversibility of Zn deposition/dissolution was significantly improved (Figure 7i). The results show that the Zn//Zn symmetric cell with the PVDF@GF composite separator achieved long-term cycling of 500 h at a capacity density of 10 mAh cm^{-2}, demonstrating outstanding stability.

4.1.3 | Biomass Modified GF Separators

The recyclability of biomass materials confirms that they are clean energy sources, meeting the needs of the current industry [97]. Carbon-rich biomass-derived nanomaterials can still maintain their nanostructural properties, featuring advantages such as self-assembly, abundant functional groups, and good stability [98]. In addition, various elements such as Fe, N, and S can be doped into biomass. This doping strategy not only produces a synergistic effect—where the porous structure of the separator, hydrophilic groups, and mechanical strength cooperate with each other to both accelerate the desolvation of Zn^{2+} and block dendrite growth—but also enhances the redox kinetics of Zn^{2+} [99]. More importantly, multielement doping induces the rearrangement of Zn^{2+} at the interface, thereby enhancing the catalytic efficiency [100]. Finally, the low cost and large-scale preparability of biomass are its advantages and also what future commercial batteries need [101].

By coating and gelifying natural chitosan (CS) on traditional GF separators, Guo et al. prepared a zinc affinity CS-GF separator, which can regulate the performance of zinc anodes [102]. The uniformly distributed CS hydrogel layer on the GF surface anchored a substantial amount of water molecules and hydrogen ions in the electrolyte, reducing their reactivity and suppressing side reactions. The functional groups of the CS-GF separator interacted with zinc ions, accelerating their diffusion and migration kinetics while mitigating the zinc dendrite growth during deposition. Additionally, the CS hydrogel layer enhanced the flatness of the GF separator, optimized its pore size distribution, and facilitated uniform zinc ion transport and deposition. The Zn//Zn symmetric battery employing this CS-GF separator demonstrated exceptional long-cycle stability and achieved a CE of 99.6%.

In addition to modifying GF separators with CS, Gou et al. investigated the ion enrichment phenomenon of algae plants, finding that the abundant functional groups in sodium alginate (SA) have high affinity for metal cations, which can enable the uniform deposition of Zn^{2+} [103]. The flux inhomogeneity will aggravate the concentration polarization and induce the protrusion, which will lead to the uneven electric field and the growth of zinc dendrite. Meanwhile, the residual active species in the solvation sheath will cause the side reaction. In the SA@GF separator, the zinc affinity groups (—OH, —COO^-) derived from SA facilitated the desolvation of hydrated Zn^{2+} and enhanced its migration capability. The hydrogel formed by SA cross-linking strengthened the separator's mechanical integrity to resist dendrite damage. The introduced Na^+ preferentially adsorbed onto the zinc anode, eliminating the tip effect and guiding Zn^{2+} to deposit uniformly (Figure 8a). Furthermore, the binding energy (BE) of $[Zn(SA)_6]^{2+}$ cluster compounds reached −54.05 eV, demonstrating that salicylate species exhibited stronger nucleophilicity than water molecules and were more readily coordinated with Zn^{2+}. This property typically optimized the solvation structure of hydrated zinc ions, thereby facilitating the desolvation process to some extent (Figure 8b).

In addition to simple biomass-modified GF separators, there are also cases of compounding them with carbon-based materials. Chen et al. synthesized nitrogen-phosphorus codoped porous carbon nanosheets (NP-PC) through in situ carbonation using chitin and phytic acid as raw materials [105]. The resulting NP-PC@GF modified separator was coated onto GF separators to address critical challenges in ZIBs, including polyiodide diffusion and dendrite growth, thereby enhancing rapid discharge capability and iodine utilization efficiency. The battery demonstrated an initial capacity of 7.8mAh cm^{-2} at 20 mA cm^{-2}, reaching 8.9mAh cm^{-2} under high iodine loading, with 56% capacity retention after 174 cycles. This provides an effective solution for developing high-performance ZIBs.

4.1.4 | Carbon Materials Modified GF Separators

Carbon materials, specifically graphene, exhibit high mechanical strength and excellent electrical conductivity, which lay a foundation for application in zinc anodes [106, 107]. Moreover, graphene features stable structures, which can be attributed to the tight bonding between carbon atoms [108–111]. Graphene also has a wide variety of types, such as Graphene oxide (GO), reduced graphene oxide, graphene quantum dots, vertical graphene, and so on. These materials can not only improve ionic conductivity but also produce synergistic effects with other materials to accelerate ion transfer and enhance electrical conductivity [112].

Huang et al. designed and fabricated a multifunctional Janus separator composed of a covalent organic framework (COF) layer, a commercial GF substrate, and a graphene (Gr) layer, enabling high-stability zinc-iodine batteries [104]. The COF layer, featuring abundant polar groups, and a homogeneous open-channel mesoporous structure, ensured uniform Zn^{2+} flux

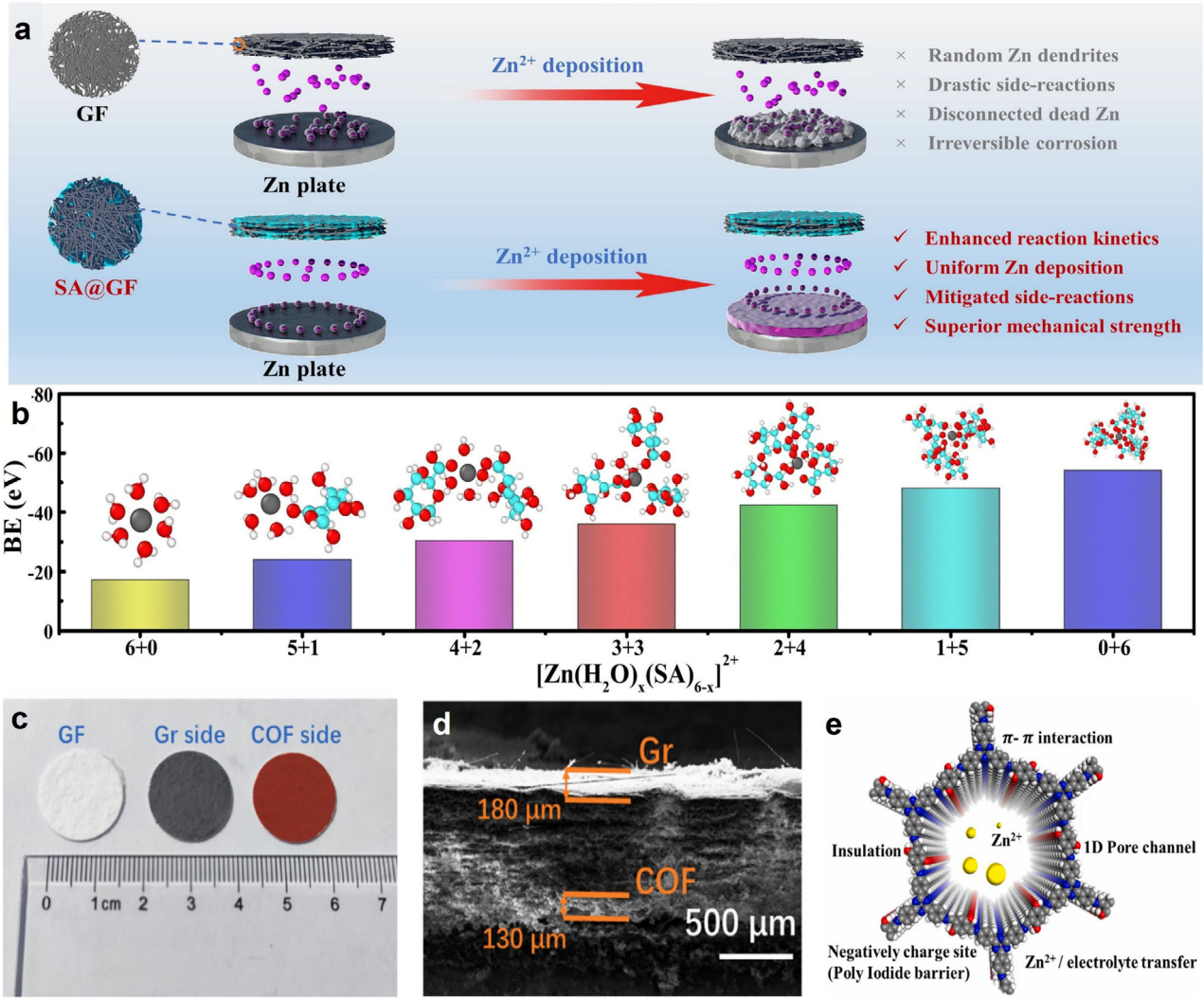

FIGURE 8 | (a) Schematic illustrations of GF and SA@GF separator on modulating Zn^{2+} deposition behavior [103]. (b) BE values of various $[Zn(H_2O)_x(SA)_{6-x}]^{2+}$ clusters ($x = 1, 2, 3...6$). Reproduced with permission [103]. Copyright 2025, Elsevier. (c) Optical picture of GF separator and TTA-DHTPA-COF@GF@Gr Janus separator [104]. (d) Cross section SEM image [104]. (e) Schematic diagram of TTA-DHTPA-COF structure. Reproduced with permission [104]. Copyright 2024, Elsevier.

while inhibiting iodide migration. The highly conductive Gr layer not only supported iodide loading but also effectively activated the redox kinetics of iodine species. The GF separator exhibits excellent uniformity as shown in Figure 8c, while cross-sectional SEM images clearly demonstrate the thickness distribution of modified materials, further confirming the uniform dispersion of COF and Gr (Figure 8d). Materials with ordered porous structures can physically block polyiodides, while chemical adsorption inhibits the shuttle effect through the chemical interaction between triazine groups and hydroxyl groups. The synergistic effects of these multifunctional properties enabled TTA-DHTPA-COF to demonstrate outstanding electrochemical performance as a modified separator material for zinc-iodine batteries. This breakthrough not only provides innovative approaches for separator design but also enhances our understanding of the relationship between COFs and high-energy-density batteries (Figure 8e).

GO is rich in oxygen-containing functional groups [113]. In addition, its good hydrophilicity, large specific surface area, and excellent adsorption performance make it stand out among many materials [114]. Chen et al. developed a multifunctional Janus separator combining organic and inorganic materials using commercial GF as the separator, which effectively inhibited zinc dendrite growth and enhanced the reversibility of zinc anodes [115]. The functional layer of this separator featured a dense microporous structure that restricts ion diffusion, while the graphene oxide-titanium dioxide (GO-TiO_2) filler promotes epitaxial deposition of Zn^{2+}. Deng et al. embedded conductive PANI as a support matrix into vanadium pentoxide hydrate (PAVO) to stabilize the cathode structure [116]. Simultaneously, GO was modified onto the GF separator surface via electrospinning and laser reduction, effectively suppressing zinc dendrite growth. The resulting battery demonstrated outstanding electrochemical performance: a specific capacity of 362 mAh g^{-1} at 0.1 A g^{-1}, maintaining high-rate capability of 280 mAh g^{-1} at 10 A g^{-1}, and achieving 74% capacity retention after 4800 cycles at 5 A g^{-1}.

4.1.5 | Polar Materials Modified GF Separators

Modified GF separators with polar materials combines structural optimization and synergistic performance advantages: polar

groups can reconstruct the hydrogen bond network of the electrolyte and suppress HER while constructing ordered ion transport channels to accelerate Zn^{2+} migration efficiency and significantly reduce charge transfer resistance; its strong polarity enables specific interactions with Zn^{2+}, guiding uniform ion distribution and directional deposition, effectively inhibiting zinc dendrite growth and "dead zinc" formation, and improving the reversibility of Zn anode deposition/dissolution; targeting the shuttle effect caused by polysulfides, polyiodides, and so on, polar materials can block the loss of active materials through strong adsorption while optimizing the separator's surface wettability and mechanical stability to ensure structural integrity during long-term battery cycling [117]. This modification strategy achieves the integration of multiple functions (e.g., ion regulation, side reaction suppression, and structural stability) through a single material, providing an efficient and feasible solution for the design of high-performance separators for ZIBs [118].

Lv et al. designed a TiO_2-coated separator to mitigate interfacial corrosion and passivation reactions, thereby enabling the development of high-performance ZIBs [119]. TiO_2 was modified on the surface of GF via a sol–gel method, followed by heat treatment and drop-casting onto the GF substrate (Figure 9a). Furthermore, the influence of the loading amount and crystal phase of the TiO_2 coating on the separator modification effect was thoroughly investigated. The results demonstrated that Zn symmetric cells employing the anatase TiO_2-modified GF separator (A-TiO_2@GF) exhibited superior Zn^{2+} ion transport kinetics in a mild $ZnSO_4$ electrolyte, ensuring long-term cycling stability and promoting uniform Zn deposition. In addition, the anatase TiO_2 coating showed significantly reduced HER activity, which can effectively inhibit H^+ ion migration, thereby minimizing interfacial corrosion and HER side reactions.

In addition to using simple polar materials, combining polar and nonpolar materials has provided a new idea for material exploration. Zhu et al. used ZIF-8 as the precursor to obtain polar ZnO by pyrolysis in a muffle furnace at 400°C [120]. This approach not only addressed the issue of slow redox kinetics but also suppressed the shuttle effect of polyiodides. The cyclic voltammetry (CV) curve of the modified separator exhibits narrower and more distinct peaks, which reflects its higher reversibility and lower polarization behavior (Figure 9b-c). This confirms that the polar material accelerates the conversion of iodine species and enhances the rate of redox kinetics.

4.1.6 | Modification of GF Separators with Other Materials

Reports on organic materials modified GF separators are relatively limited, so a brief example is provided here. Li et al. developed L-Alanine composite GF(LA@GF) through thermal treatment of GF with L-alanine and sodium hydroxide solution [122]. The synergistic interaction between introduced -NH_2 and -COOH functional groups of L-alanine facilitated uniform zinc ion deposition. Specifically, the -NH_2 group acted as an "ion pump" for zinc ion transport, enhancing migration kinetics and significantly improving both zinc ion migration numbers and exchanging current density in the modified separators. Meanwhile, the -COOH group formed hydrogen bonds with water molecules, accelerating the desolvation process of zinc hexahydrate ions.

Liu et al. successfully developed a functionalized Janus separator by coating GF with elosite nanotubes (HNTs) (Figure 9d) [121]. The electronegativity difference between the inner and outer surfaces of HNTs endowed the HNT-GF separator with ion screening properties, significantly enhancing zinc ion migration (t_{Zn}^{2+} = 0.71). This HNT-GF separator functions as an interfacial "ion comb," regulating zinc ion flux and enabling multisite progressive nucleation, ultimately reducing nucleation overpotential and promoting uniform zinc ion deposition. Notably, the adsorption energy of SO_4^{2-} on the inner surface of HNTs (−1.125 eV) was higher than that on the outer surface (−0.391 eV), while the outer surface exhibited stronger adsorption capacity for Zn^{2+} and H^+ compared to the inner surface. Computational results indicated that the inner surface of HNTs effectively captured SO_4^{2-}, whereas the outer surface's favorable affinity for cations created an "ion comb" effect, homogenizing ion flux to facilitate Zn^{2+} desolvation and uniform nucleation (Figure 9e,f).

4.2 | Novel Separators

4.2.1 | Cellulose Separators

GF exhibits excellent compatibility with aqueous electrolytes, but its poor mechanical properties and large pore sizes lead to severe zinc dendrite growth, which can cause short circuits in batteries [123]. Cellulose-based separators (CF), as natural organic polymers, offer several advantages, including high mechanical strength, hydrophilicity, insulation properties, and cost-effectiveness. Compared to GF separators, CF separators have a denser pore structure, abundant functional groups, and excellent ionic conductivity, along with higher tensile strength and modulus. Moreover, CF separators not only reduce the nucleation potential but also suppress unwanted side reactions [124]. Thus, cellulose-based separators have become a promising separator material for ZIBs.

Li et al. proposed optimizing molecular aggregation states by regulating the loosening effect of intermolecular hydrogen bonds, thereby preparing high-performance robust cellulose separators [125]. The preparation process used wood pulp as raw materials, followed by being dissolved in 1-allyl-3-methylimidazolium chloride. After completing cellulose dissolution, DMSO was introduced as a cosolvent to promote molecular uniform dispersion and reduced the system viscosity, ensuring uniformity during casting. Subsequently, anhydrous ethanol was used as a regeneration agent to suppress excessive rearrangement and reconstruction of hydrogen bonds between cellulose chains during regeneration. In contrast, when deionized water was used as the regeneration agent under the same synthesis conditions, a mildly disordered regenerated cellulose separator (LDCS) was obtained, exhibiting stronger hydrogen bond interactions between cellulose chains (Figure 10a). DFT calculations showed that the dissociation energies of Zn^{2+} on the-OH groups at C6, C4, and C2 positions of cellulose were −34.1, −13.9, and −18.2 kcal mol^{-1}, respectively (Figure 10b), reflecting the differences in interaction strength between Zn^{2+} and hydroxyl groups at different carbon positions. Molecular dynamics (MD) simulations demonstrated Zn^{2+} chain transport within 15 ns in both HDCS and LDCS (Figure 10c). In LDCS, Zn^{2+} transport was unevenly hindered by strong hydrogen bond stacking in the

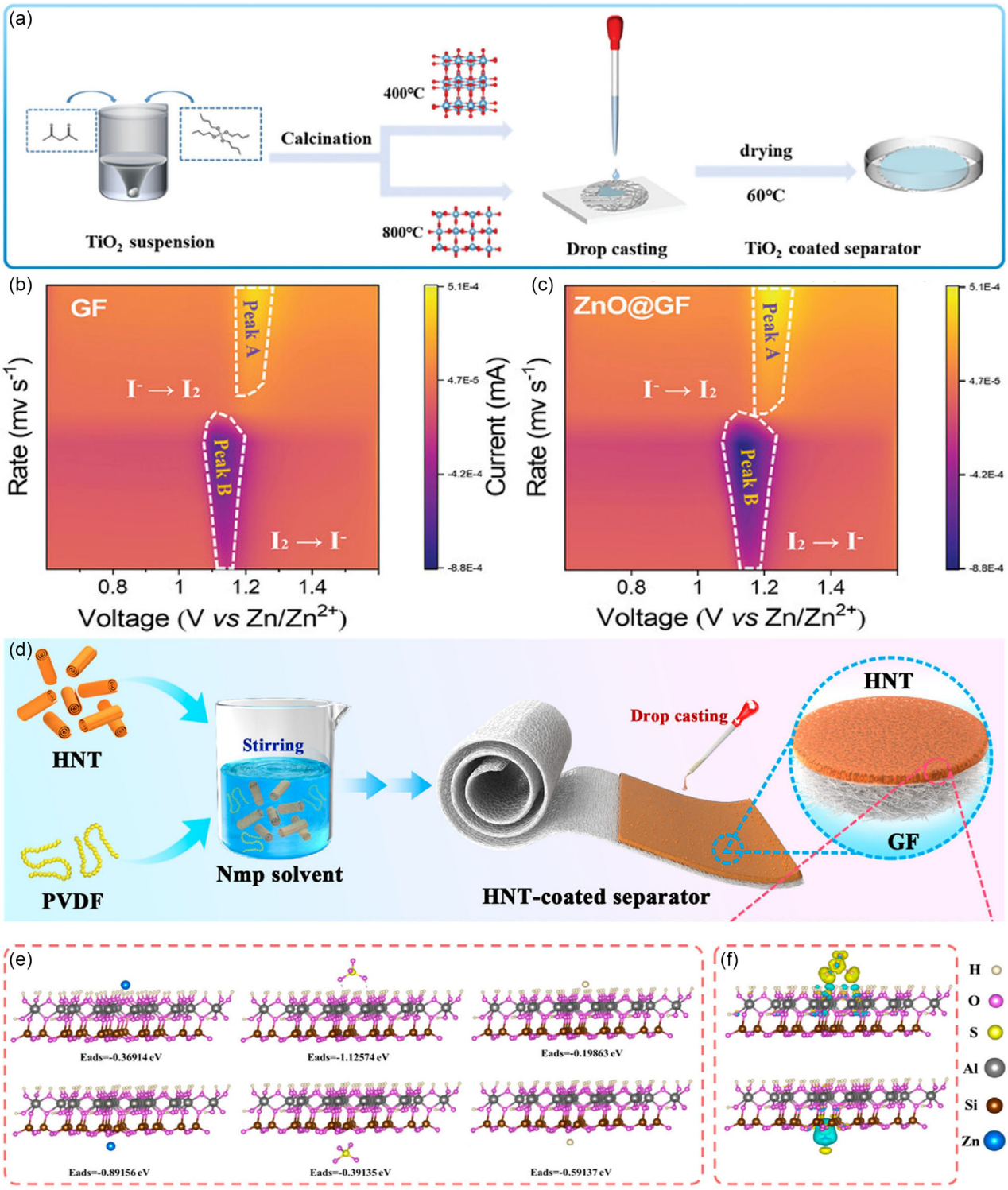

FIGURE 9 | (a) Schematic of the preparation of the A-TiO_2@GF Separator [119]. Copyright 2024, Wiley-VCH. Contour maps of CV curves for batteries with (b) GF and (c) ZnO@GF modified separators at different scan rates. Reproduced with permission [120]. Copyright 2025, Wiley-VCH. (d)Schematic diagram describing the preparation process of the HNT-GF separator and ion-sieving mechanism of HNT [121]. (e) Structural models for calculating the adsorption energies of Zn^{2+}, SO_4^{2-}, and H^+ on the inner/outer surfaces of HNTs [121]. (f) Charge density differences triggered by SO_4^{2-} adsorption on the inner surface and Zn^{2+} adsorption on the outer surface (cyan stands for charge depletion, yellow for charge accumulation). Reproduced with permission [121]. Copyright 2024, American Chemical Society.

molecular chains; in HDCS, the loosening effect of hydrogen bonds reduced Zn^{2+} diffusion resistance, facilitating uniform transport and suppressing zinc dendrite formation.

On the basis of optimizing cellulose separators by regulating hydrogen bonds, Wang et al. proposed an interface strategy for all-cellulose separators, utilizing the synergistic chemical

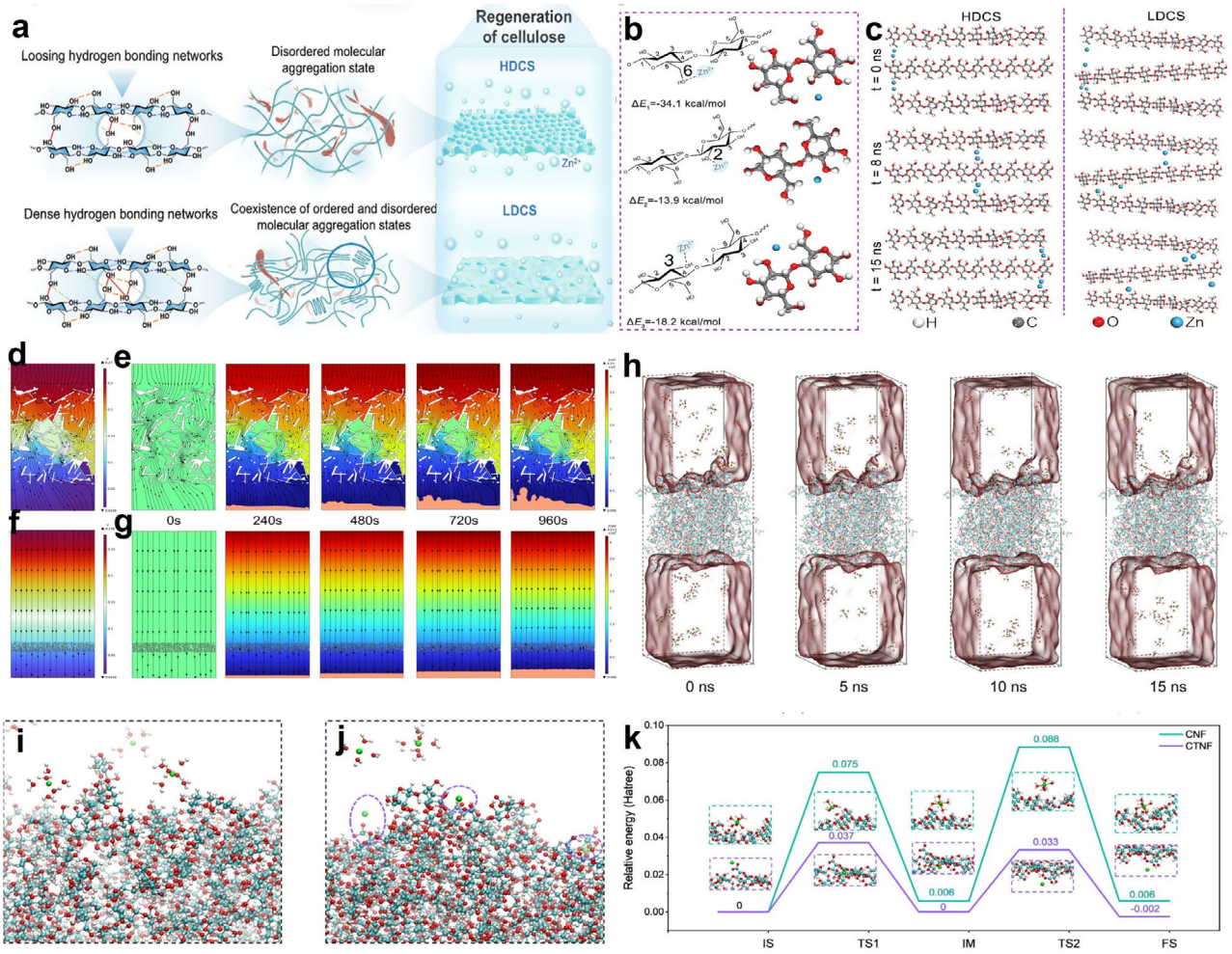

FIGURE 10 | (a) Schematic diagram of the preparation processes [125]. (b) Dissociation energies of Zn^{2+} de-coordinating at different positions of the glucose molecular chain [125]. (c) Structural snapshots from MD simulations of a fast-moving Zn^{2+} transporting in HDCS and LDCS separator within 15 ns. Reproduced with permission [125]. Copyright 2025, Wiley-VCH. (d) electric field and (e) Zn^{2+} concentration field during the Zn deposition process coupled with the GF separator [126]; (f) electric field and (g) Zn^{2+} concentration field during the Zn deposition process coupled with the CTNF separator [126]. (h) 3D view (within a thickness of 50 Å) of Zn^{2+} distribution evolution at the electrolyte/CTNF interface [126]. (i) the interaction between the electrolyte and the CNF chains; (j) the interaction between the electrolyte and the CTNF chains [126]. (k) The relative energy and computational models (insets) of Zn^{2+} migrating along the CNF chain (above) and CTNF chain (below). Reproduced with permission [126]. Copyright 2025, Elsevier.

regulation of hydroxyl and carboxyl groups to control zinc deposition interfaces, achieving highly stable zinc anodes [126]. For the designed cellulose separator, carboxyl groups interacted electrostatically with zinc ions while the hydroxyl network captured water molecules through hydrogen bonding. The synergistic network combining electrostatic interactions and hydrogen bonding effectively promoted zinc ion generation, transport, and dissolution, leading to dendrite-free zinc deposition. Through COMSOL Multiphysics (COMSOL) simulations, the electric field distribution and Zn^{2+} flux characteristics during zinc deposition were investigated, comparing the performance of GF separators with cellulose separators (CTNF). The GF separator exhibited disordered internal electric field distribution and uneven Zn^{2+} flux, which promoted zinc dendrite formation and growth (Figure 10d,e). In contrast, the uniform nanoporous structure of the CTNF separator achieved even distribution of both electric field and ion flux, effectively suppressing zinc dendrite growth (Figure 10f,g). Observations of hydrated zinc ions within CTNF molecular chains revealed desolvated Zn^{2+} at the interface (Figure 10h). The abundant hydroxyl groups in CNF chains formed strong hydrogen bonds with water molecules, affecting the solvation structure $[Zn(H_2O)_6]^{2+}$ (Figure 10i). The introduction of carboxyl groups enhanced CTNF chain affinity for Zn^{2+}, partially disrupting its solvation sheath and promoting interface desolvation (Figure 10j). The results of the migration energy barrier of Zn^{2+} in cellulose chains showed that the energy required for Zn^{2+} to overcome the migration steps in CNF chains was 0.075, 0.069, 0.082, and 0.082 Hartree, respectively, while the strong interaction between the carboxyl group and Zn^{2+} in hydrated Zn^{2+} can accelerate the desolvation process of hydrated Zn^{2+} in CTNF chains (Figure 10k).

4.2.2 | Polyolefin Separators

As a traditional separator material of ZIBs, polyolefin separators, such as polypropylene (PP) and polyethylene (PE), integrate structural characteristics and practical advantages: Their regular porous structure can construct efficient ion transport channels, facilitating the rapid migration of Zn^{2+} and reducing battery

internal resistance [127, 128]; they exhibit excellent chemical stability, resisting electrolyte corrosion and effectively suppressing the occurrence of side reactions such as HER to ensure battery cycling safety; with outstanding mechanical strength, they can withstand the puncture risk caused by zinc dendrite growth and maintain structural integrity during long-term battery cycling; meanwhile, they possess the characteristics of low cost, large-scale manufacturability, and good processing compatibility, meeting the requirements of commercial production. In addition, the surface of PP separators can be easily modified via grafting, coating, or other methods to introduce polar groups or functional fillers, which further optimizes ion selectivity and interfacial compatibility, thereby expanding their application potential in high-performance ZIBs.

Zhu et al. developed a PP-g-AA separator featuring hydrophobic/hydrophilic domains [129]. The PP matrix partially blocked water molecules to minimize side reactions, while the carboxyl functional groups in the grafted acrylic acid (AA) effectively regulated the interfacial electric field and Zn^{2+} concentration field, significantly enhancing zinc ion flux homogenization for dendrite-free deposition. In Zn//Zn symmetric cells, GF separators showed no significant fluctuations in charge transfer impedance during discharge, with only a slight post-charging decline (Figure 11a) matching the overall resistance trend. In contrast, PP-g-AA separators demonstrated substantial resistance reduction after cycling (Figure 11b), confirming their role in facilitating zinc ion interfacial transport. DFT analyses revealed that carboxyl groups form hydrogen bonds with water molecules, effectively reducing the free water content and minimizing Zn^{2+}-water contact in the electrolyte to suppress side reactions (Figure 11c,d).

Beyond the functional modification of polypropylene separators via acrylic acid grafting, titanium dioxide grafting on polyethylene separators has also emerged as an effective strategy for regulating zinc deposition behavior and optimizing separator performance in ZIBs. Yu et al. developed a composite film

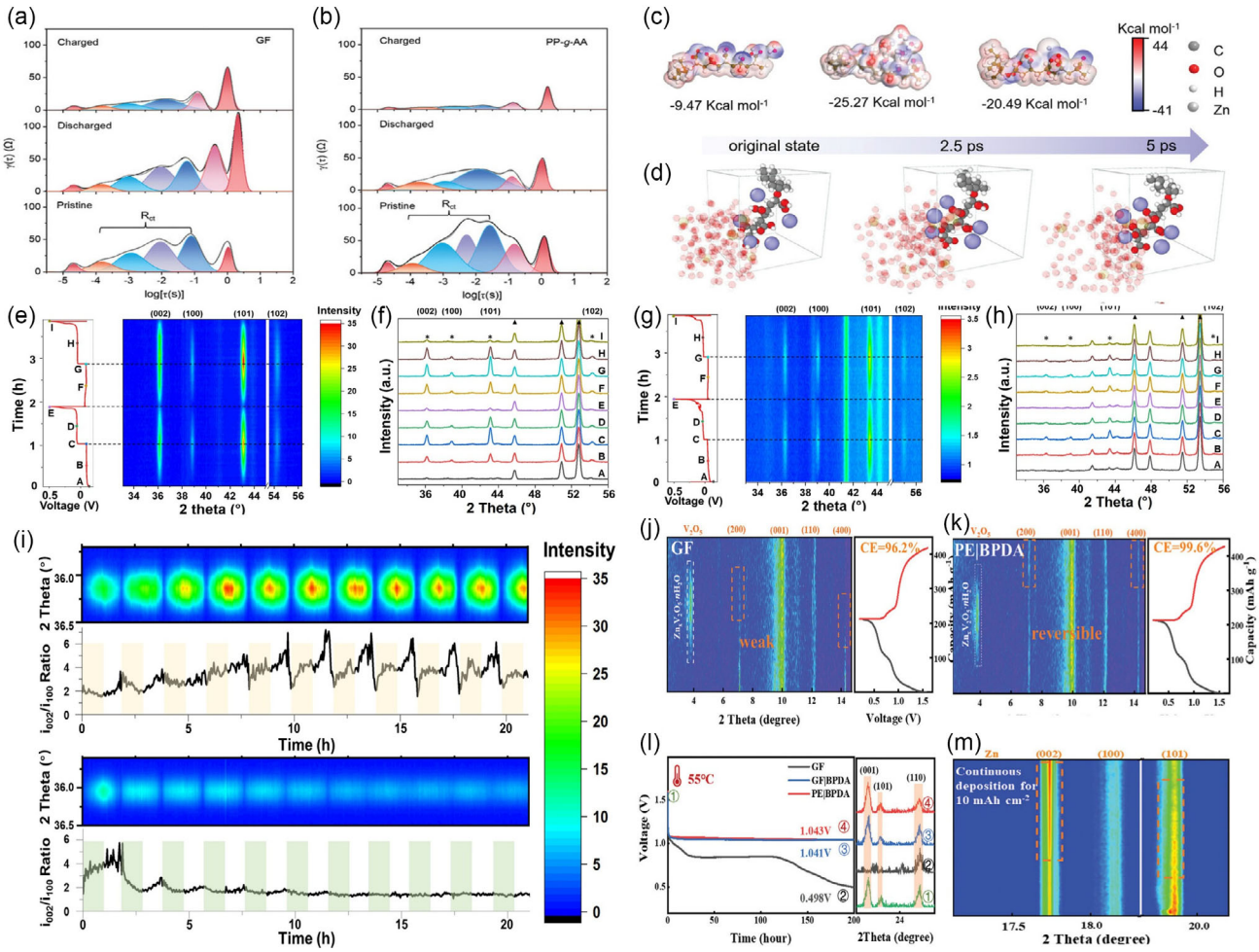

FIGURE 11 | The DRT plots correspond to the Zn//Zn symmetric cells with GF (a) and PP-g-AA separator (b), respectively [129]. (c-d) MESP isosurface plots between a PP-g-AA chain and different species of Zn^{2+} and H_2O. Reproduced with permission [129]. Copyright 2024, Wiley-VCH. (e-h) In situ XRD patterns of the deposited Zn with the (e and f) TiO_2-PE and (g and h) GF/A separator [130], (i) The variation of (002) peak intensity and i_{002}/i_{100} ratio of the deposited Zn in the initial 11cycles with the TiO_2-PE and GF/A separators. Reproduced with permission [130]. Copyright 2024, Elsevier. (j,k) The transmission-mode Operando XRD pattern of the V_2O_5 cathode with GF or PE|BPDA separators as reference to the pristine Zn foil [131]. (l) OCV profiles of the Zn//V_2O_5 cell model with GF, GF|BPDA, and PE|BPDA separators at the oxidized charged state, and corresponding XRD patterns of the V_2O_5 cathode before and after 200 hr static idling process [131]. (m) The real-time evolution of the crystallographic orientation of Zn deposits during the continuous plating process till 10 mAh cm^{-2}. Reproduced with permission [131]. Copyright 2024, Wiley-VCH.

(TiO_2-PE) by grafting TiO_2 onto PE separators [130]. This separator exhibited excellent hydrophilicity, with its small pore size promoting uniform zinc deposition. XRD analyses of the crystal structures revealed consistent peak intensity trends across different separators, though absolute intensity variations suggested that separator properties influence zinc deposition yield and crystal growth density. The TiO_2-PE system demonstrated higher zinc peak intensity, indicating superior uniformity in zinc deposition (Figure 11e-h). During cycling, the sustained strengthening of (002) orientation in the TiO_2-PE system resulted in a progressively planarized and dense zinc deposit, effectively suppressing dendrite growth. In contrast, the GF/A system exhibited disordered orientation, leading to dendrite accumulation and battery failure (Figure 11i).

In addition to the strategy of titanium dioxide grafting modification, researchers have further improved the comprehensive performance and service stability of ZIB separators by fabricating ultra-thin functionalized separators via molecular design. Xue and coworkers developed a 9 μm-thick molecularly designed thin-layer separator that simultaneously achieved long storage lifespan, excellent cycling stability, and high actual energy density for ZIBs [131]. Specifically, a mechanical-arm-controlled spraying technique was employed to anchor biphthalic anhydride on the cathode surface of PE. This modification significantly suppressed vanadium's spontaneous dissolution and shuttle behavior during both dynamic cycling and static high-temperature storage. After charge–discharge cycles with the GF separator model, the slight reduction in crystal intensity indicated irreversible structural damage. In stark contrast, the cathode's characteristic peak intensity of the modified separator showed almost no significant change during cell operation (Figure 11j-k). The self-discharge tracking shows that the structure of GF and cathode collapse, while the modified PE maintains stable crystal structure (Figure 11l). The real-time monitoring of crystal evolution in the continuous deposition process shows that the peak intensity gradually increases, which confirms that the zinc deposit has the characteristics of preferential horizontal structure and dendrite protrusion inhibition (Figure 11m).

4.2.3 | Biomass-Based Separators

Biomass has gained favor in ZIBs due to its advantages, such as low cost, abundant sources, and good compatibility [132]. Additionally, their physicochemical properties are highly compatible with ZIBs. The unique polar functional groups in biomass can provide binding sites, and the hydrophilicity of these functional groups allows for regulation of water activity. Biomass materials can not only be easily converted into carbon nanomaterials, but also the enriched molecular structures endow them with inherent advantages such as flexibility and self-healing properties [133].

These excellent properties render biomass materials ideal candidates for ZIBs, and researchers have accordingly developed a variety of high-performance biomass-based separators and verified their modification effects. Wang and coworkers developed a chitin nanofiber separator via a simple, low-cost, and scalable strategy [134]. As shown in Figure 12a, the chitin extracted from shrimp and crab shells was oxidized to obtain the 2,2,6,6-tetramethyl-piperidin-1-oxyl (TEMPO)-oxidized chitin (TCh) nanofiber suspension. The TCh nanofiber suspension was then processed through a wet flat-bottom milling process for mass production. This separator featured abundant zinc-friendly functional groups and uniform nanopores, facilitating the desolvation of Zn^{2+}. The zinc anode with GF exhibited a Zn^{2+} tip effect, accelerating dendrite growth. In contrast, TCh's smaller pores and denser microstructure promoted uniform Zn^{2+} deposition (Figure 12b). Ma et al. developed a novel oxygen-functionalized biomass bamboo separator (BM) designed to suppress water molecule activity [135]. The separator featured a unique multilayered two-dimensional sandwich structure that facilitated rapid ion diffusion. Its oxygen-functional groups formed hydrogen bonds with water molecules, effectively converting free water into bound states. Both the density and energy of hydrogen bonds between BM and water molecules surpass those observed in GF systems, demonstrating BM's superior interfacial affinity for water (Figure 12c-d). DFT calculations confirm stronger interactions between BM and water molecules, resulting in higher binding energy (Figure 12e). Unlike GF's uneven electric field distribution, BM exhibits uniform electric field and current density (Figure 12f-i). These findings indicate that BM separators capture water molecules through hydrogen bonding, transforming them from free to bound states—a clear advantage over conventional separators.

Beyond the BM separator, researchers have also applied carbonyl-functionalized biosynthetic cellulose separators to ZIBs, which further enables uniform Zn deposition/stripping on the zinc anode and efficient suppression of zinc dendrites. Zhang et al. enhanced the uniform deposition/stripping of zinc anodes in ZIBs and effectively suppressed zinc dendrite growth by modifying biosynthetic cellulose separators with carbonyl functional groups (CCM) [136]. This modification weakens the interaction between the polymer framework and zinc ions, thereby improving zinc-ion migration efficiency. The modified separator has a thickness of only 21 μm. The assembled zinc symmetric cells achieved a cycle life exceeding 2800 h under conditions of 1 mA cm^{-2} and 1 mAh cm^{-2} and maintained stable cycling for 300 h even under high-load conditions of 5 mA cm^{-2} and 3 mAh cm^{-2}. Furthermore, full cells paired with sodium vanadate cathodes retained stable performance over 2000 cycles at a current density of 3 A g^{-1}. This work provides new insights into the molecular design of separators for ZIBs.

In addition to optimizing separator performance through chemical group modification, Luo et al. adopted a different approach by loading functional nanomaterials onto substrate surfaces [137]. Using a simple and low-cost filtration method, they loaded ultralight graphene oxide (GO) nanosheets onto a cellulose acetate (CA) separator to construct a GO/CA composite separator. Leveraging the small lattice mismatch between GO and zinc metal, along with the abundant hydrophilic oxygen-containing functional groups of GO, the separator guides the epitaxial electrodeposition of zinc ions along the (002) crystal plane, enabling uniform and dendrite-free zinc deposition. Zinc symmetric cells assembled with this composite separator achieved a cycle life of 500 h under high current density conditions of 10 and 1 mAh cm^{-2}, while also exhibiting a low nucleation overpotential of 89 mV and a CE exceeding 96%.

Taking the research a step further, Ma et al. drew inspiration from the anisotropic structure of natural wood to innovatively develop a biomimetic separator that combines high modulus

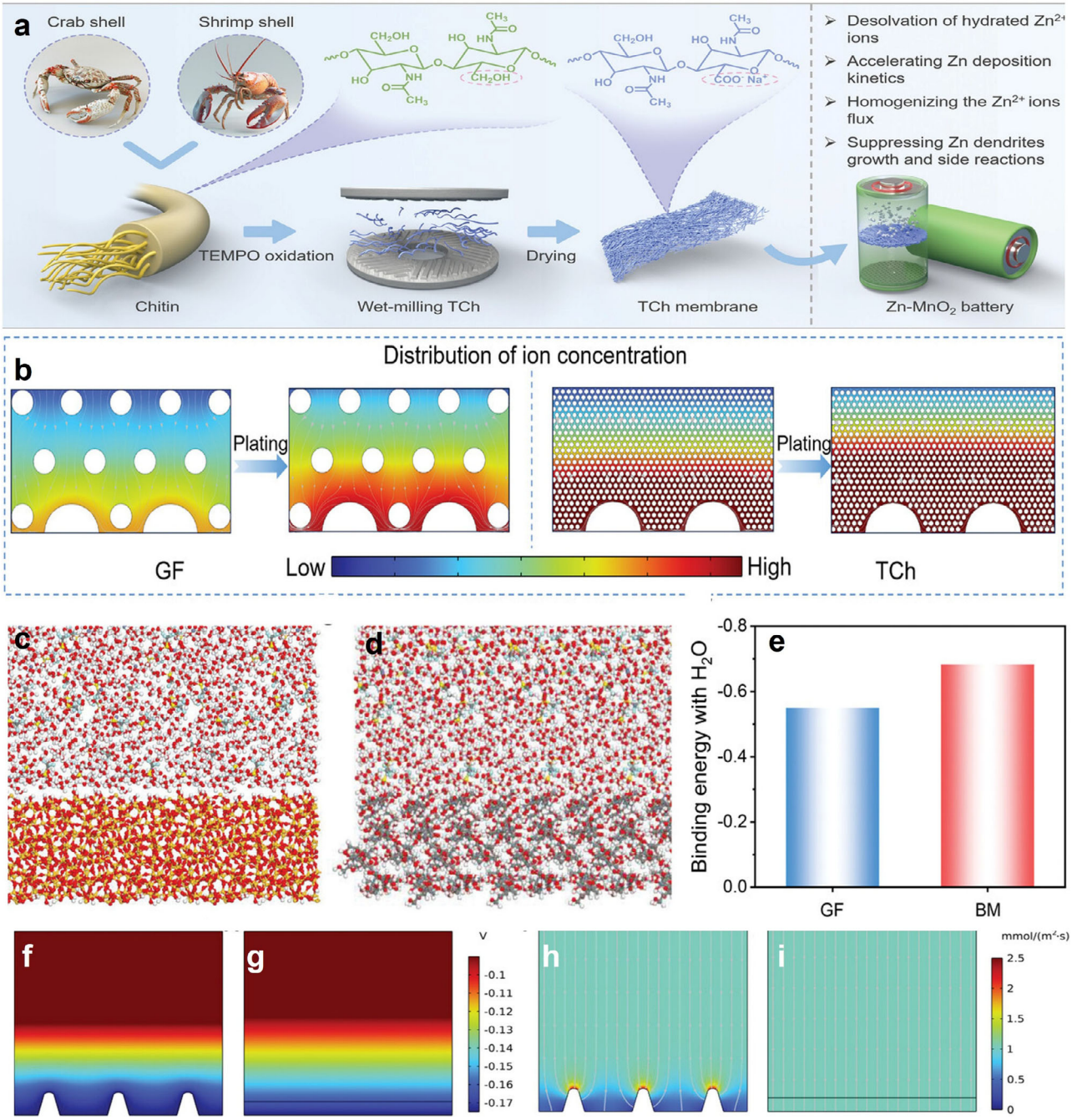

FIGURE 12 | (a) Schematic illustration of the preparation strategy for the TCh separator. (b) Ionic field simulation of GF and TCh systems. Reproduced with permission [134]. Copyright 2024, Wiley-VCH. (c) 3D snapshot of MD calculation for the interaction between GF and 1 M $Zn(OTf)_2$ solution [135]. (d) 3D snapshot of MD calculation for the interaction between BM and 1 M Zn $(OTf)_2$ solution (H, white; C, gray; O, red; F, cyan; S, yellow; Si, orange) [135]. (e) Binding energy comparison between GF-H_2O and BM-H_2O. The electrical field models are based on (f) GF and (g) BM [135]. The zinc ion concentration field models are based on (h) GF and (i) BM. Reproduced with permission [135]. Copyright 2024, Wiley-VCH.

and high ionic conductivity [138]. Using a directional freezing method, they fabricated a biomimetic anisotropic and degradable separator (V-NFC-CS) composed of nanocellulose and chitosan. With a thickness of only 23 μm, this separator achieves both a high modulus of 7.3 GPa and a high ionic conductivity of 20.5 mS cm^{-1} along the oriented direction. This design resolves the trade-off between separator thickness and dendrite resistance while overcoming the challenge of simultaneously achieving high modulus and high ionic conductivity. The vertically aligned channels within the separator help to evenly distribute current density and zinc ions, guiding zinc to deposit horizontally along the (002) crystal plane, thereby effectively suppressing dendrite growth and side reactions. As a result, zinc symmetric cells achieved stable cycling for over 1000 h under conditions of 10 mA cm^{-2} and 2 mAh cm^{-2}, while full cells paired with MnO_2 cathodes retained 96.2% capacity after 1000 cycles at 1 A g^{-1}. Moreover, the separator exhibits excellent biodegradability, offering a new solution for high-performance ZIBs.

4.2.4 | Janus Separator

Janus materials typically exhibit dual-functional properties due to the different materials on their two sides, featuring not only high mechanical strength but also excellent chemical stability [139]. Even though the two materials are interrelated and exhibit a synergistic effect, which is where their advantage lies [140, 141].

Such Janus materials with synergistic structural and performance advantages have also been widely applied in the design and modification of separators for ZIBs. Zheng et al. developed a Janus-type CF/PVA/ZrO_2 separator via vacuum filtration [142]. The interwoven cellulose fibers provided robust mechanical support to prevent dendrite penetration, while ZrO_2 nanoparticles regulated electric field distribution through the Maxwell-Wagner effect, effectively promoting homogeneous nucleation. The Young's modulus revealed that the CF/PVA/ZrO_2 separator demonstrated significantly higher mechanical properties compared to GF and CF, ensuring battery safety (Figure 13a). Furthermore, in localized electric field simulations, CF exhibited marked increases in localized electric field intensity, whereas the modified separator eliminated such increases, guaranteeing uniform zinc ion deposit (Figure 13b-c). Similarly, Wu et al. extracted wheat straw cellulose using UV-assisted degreasing, then processed it into lignin-containing NFC via ultrasonic treatment [145]. The $Ti_3C_2T_x$ layer was fabricated through conventional etching processes (Figure 13d). Sequential vacuum filtration of both components yielded a bidirectional heterogeneous Janus MN separator with a 32 μm thickness, exhibiting 215.3 MPa strength and 8.8 GPa modulus. The $Ti_3C_2T_x$ layer's Maxwell-Wagner effect and low lattice mismatch properties facilitated Zn^{2+} migration, accelerated desolvation, enhanced interfacial charge transport, reduced nucleation overpotential, promoted uniform zinc deposition, and suppressed side reactions.

4.2.5 | Nafion-Assembled Separators

Nafion, a perfluorosulfonic acid (PFSA) polymer separator, boasts unique advantages in ZIBs while facing unresolved contradictions, all rooted in its distinctive molecular structure [146, 147]. Its phase-separated architecture—comprising a hydrophobic polytetrafluoroethylene (PTFE) backbone and

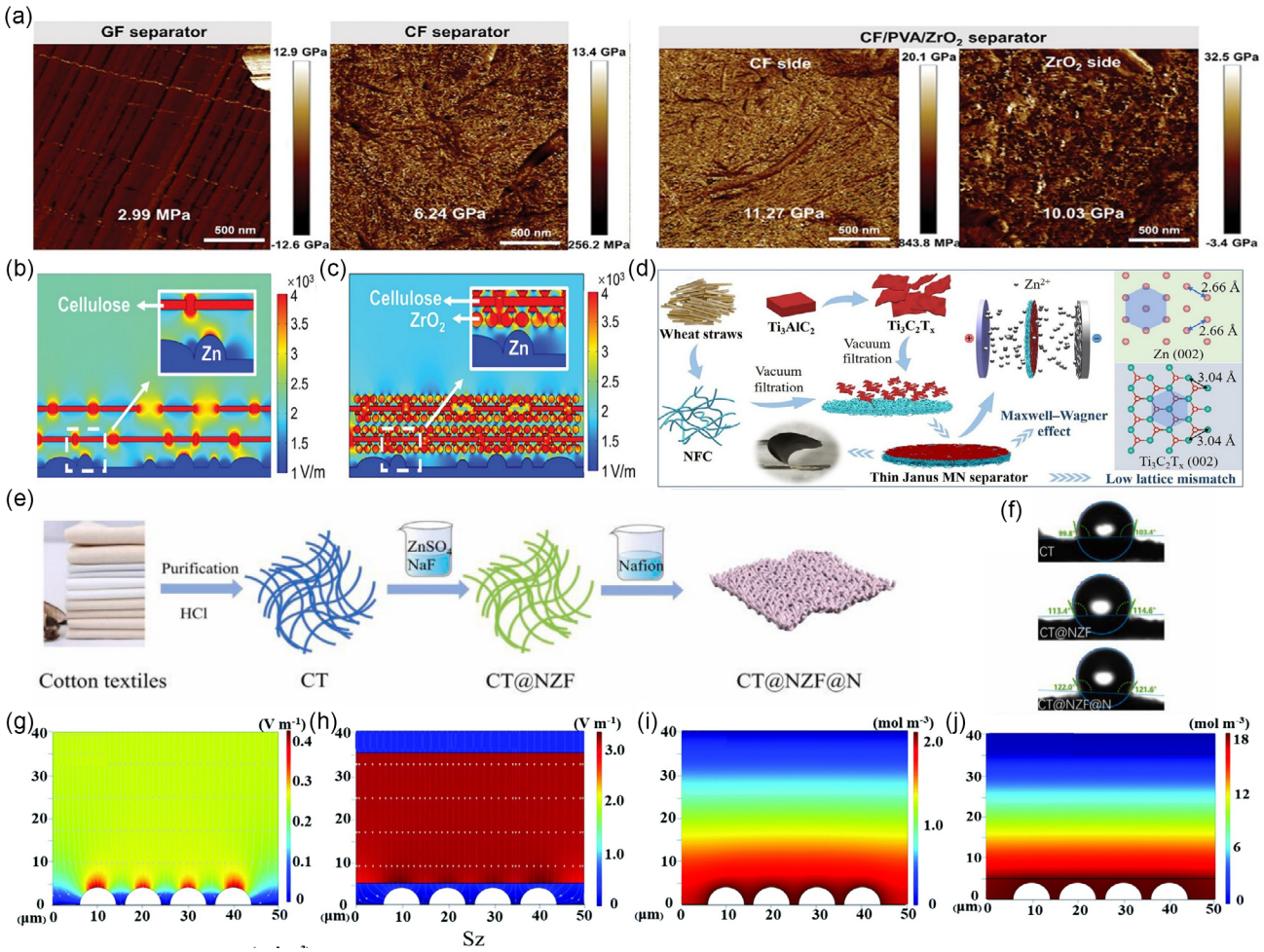

FIGURE 13 | (a) GF separator, CF separator, CF side, and ZrO_2 side of CF/PVA/ZrO_2 separator. Simulated electric field distribution near the Zn anode in contact with (b) a CF separator and (c) a CF/PVA/ZrO_2 separator [142]. (d) Schematic diagram of the preparation and benefits of MN separator. Reproduced with permission [142]. Copyright 2024, Wiley-VCH. (e) Schematic illustration of preparing the functional separators [143]. (f) Contact angle measurements of three separators. Reproduced with permission [143]. Copyright 2023, Elsevier. The electrical field models based on the GF separator (g) and (h) Zn-Nafion separator [144]. The zinc ion concentration field models based on the GF separator and (i and j) Zn-Nafion separator. Reproduced with permission [144]. Copyright 2021, Royal Society of Chemistry.

TABLE 1 | Performance Comparison and Summary of Metal–Organic Frameworks and Polymer-Modified GF Separators.

Separator Materials	Main function	Average CE [mA cm^{-2}, mAh cm^{-2}]	Cycling lifespan [mA cm^{-2}, mAh cm^{-2}]	References
ZIF-8@GF	Inhibit dendrite formation	300 cycles, 100% (2,1)	2300 h (0.5,0.25)	[80]
H-F-ZIF@GF	Rapid reaction kinetics	300 cycles, 99.5% (10,2)	300 h (10,2)	[81]
UiO-66@GF	Corrosion preventive	350 cycles, (2,1)	1650 h (2,1)	[84]
UiO-S2@GF	Inhibit of hydrogen evolution reaction	1000 cycles, (2,1)	3450 h (3,1)	[85]
PI@GF (Dip coating)	Inhibit dendrite formation	1000 cycles, 99.79%	6000 h (1,1)	[91]
PI@GF (Drop casting)	Inhibit of hydrogen evolution reaction	1700 cycles, 99% (1,0.5)	1280 h (1,1)	[92]
PZ@GF	Inhibit dendrite formation	100 cycles, 99% (1,1)	2000 h (0.5,0.5)	[93]
PAN@GF	Inhibit dendrite formation	80 cycles, 99% (10, /)	800 h (0.283, /)	[94]
GFNs-PVDF@GF	Inhibit dendrite formation	650 cycles, 100% (1, 0.5)	1800 h (1,1)	[95]
PVDF@GF	Corrosion preventive	400 cycles, 99.7% (5,1)	500 h (10,1)	[96]

TABLE 2 | Performance comparison and summary of GF separators modified by biomass, polar materials, and carbon materials, and so on.

Separator materials	Main function	Average CE [mA cm^{-2}, mAh cm^{-2}]	Cycling lifespan [mA cm^{-2}, mAh cm^{-2}]	References
SA@GF	Fast desolvation	600 cycles, 99.5% (2,1)	1230 h (1,1)	[103]
TTA-DHTPA-COF@GF@Gr	Rapid reaction kinetics	270 cycles, 98% (5, /)	600 h (10, /)	[104]
A-TiO_2@GF	Inhibit of hydrogen evolution reaction	880 cycles, 98.9% (2,1)	1400 h (1,1)	[119]
ZnO@GF	Rapid reaction kinetics	2600 cycles, 100% (5, /)	/	[120]
HNTs@GF	Rapid reaction kinetics	950 cycles, 99.7% (1,1)	3000 h (1,1)	[121]

TABLE 3 | Performance and summary comparison of novel separator materials.

Separator Materials	Main function	Average CE [mA cm^{-2}, mAh cm^{-2}]	Cycling lifespan [mA cm^{-2}, mAh cm^{-2}]	References
HDCS	Fast desolvation	400 cycles, 99.03% (2,0.5)	1000 h (1,1)	[125]
CTNF	Inhibit dendrite formation	300 cycles, 99% (1,1)	1800 h (0.5,0.5)	[126]
TCh	Rapid reaction kinetics	600 cycles, 98.9% (1,1)	2500 h (1,1)	[134]
BM	Fast desolvation	300 cycles, 99% (1,1)	1000 h (1,1)	[135]
CCM	Rapid reaction kinetics	700 cycles, 100% (1,1)	2800 h (1,1)	[136]
GO/CA	Inhibit dendrite formation	/	300 h (5,1)	[137]
V-NFC-CS	Inhibit dendrite formation	600 cycles, 99% (1,1)	1000 h (10,2)	[138]
CF/PVA/ZrO_2	Inhibit dendrite formation	150 cycles, 99.18% (/,0.6)	400 h (6,3)	[142]
CT@NZF@N	Inhibit dendrite formation	650 cycles, 99.1% (0.5,0.5)	300 h (0.5,0.5)	[143]
Zn-Nafion	Rapid reaction kinetics	130 cycles 97.8% (5,0.5)	553 h (0.5,5)	[144]

hydrophilic side chains bearing -SO_3H—endows it with dual functionalities. First, the -SO_3H enables ion exchange with Zn^{2+}, which reduces the desolvation energy barrier of Zn^{2+} and guides its uniform deposition, thereby promoting the formation of a smooth zinc deposition layer. Second, the hydrophobic PTFE backbone inhibits excessive penetration of water molecules, mitigating water-induced side reactions. However, a critical contradiction persists: the approximately 4 nm ion channels within Nafion, while facilitating selective cation transport, still permit partial passage of small molecules such as H_2O

and SO_4^{2-}. This leakage triggered interfacial side reactions at the zinc anode: water molecules penetrating through the channels induce HER, and migrating SO_4^{2-} can react with Zn^{2+} and OH^- to form by-products like $Zn_4(OH)_6SO_4{\cdot}5H_2O$. These side reactions not only lower the CE but also accelerate the growth of zinc dendrites, posing challenges to the long-term stability of ZIBs.

To address this inherent structural contradiction of pure Nafion and leverage its superior ion regulation performance, researchers have proposed a modified Nafion-based composite separator strategy by combining it with inorganic fluoride-modified biomass substrates. Guo et al. pretreated cotton fabric with 2 mol L^{-1} hydrochloric acid to remove all impurities, which fabricated fluorine-decorated cotton textiles (CT) separators for stabilizing Zn metal anodes [143]. The CT separator was then immersed in $ZnSO_4$ and NaF solutions to facilitate the growth of inorganic fluorides on the separator, yielding the CT@NZF intermediate. Subsequently, the CT@NZF was immersed in Nafion solution and dried to successfully prepare the organic–inorganic composite-layer-modified CT@NZF@N separator (Figure 13e). The CT@NZF@N exhibits a larger hydrophilic angle, demonstrating its high hydrophobicity (Figure 13f). Additionally, Nafion effectively regulated zinc deposition, reducing dendrite formation while promoting the desolvation of Zn^{2+}. The results indicate that the zinc symmetric battery achieved a lifespan of 300 hr, offering cost-effectiveness and scalability for other battery types.

Similarly, Wu et al. developed a Zn-Nafion separator [144]. On the anode side, the Zn-Nafion separator created a uniform electric field and Zn^{2+} concentration field, suppressing zinc dendrites and enabling lower polarization and longer cycling life for Zn//Zn symmetric batteries. On the cathode side, it enhanced H^+/Zn^{2+} coembedding with H^+ reactions, converting the byproduct $ZnSO_4(OH)_6{\cdot}nH_2O$ into a dense SEI layer to protect the cathode from dissolution. When using GF separators, uneven electric field distribution leads to nonuniform Zn^{2+} distribution (Figure 13g-h). However, Zn-Nafion not only achieves uniform electric field distribution but also reduces the battery's concentration gradient (Figure 13i-j). Additionally, the superior mechanical properties of Zn-Nafion separators enable better recycling and cost savings.

This section systematically introduces the two core strategies of separator engineering. The first is the surface modification of commercial GF separators: by loading functional materials such as MOFs, polymers, biomass, and carbon materials, the ion selectivity, mechanical strength, and interfacial compatibility of the separators are optimized, thereby suppressing dendrite growth and side reactions. The second is the development of novel separators including cellulose-based, polyolefin-based, biomass-derived, and Janus-structured ones. Leveraging their inherent structural advantages and functional properties, these novel separators construct efficient transport channels and achieve long-cycle stable operation of zinc anodes. Both strategies provide critical support for high-performance ZIBs through the precise regulation of the physical structures and chemical properties of separators.

5 | Conclusions and Prospects

As a critical component, separators not only physically isolate electrodes but also enable active control of zinc deposition and inhibition of side reactions through engineering design, serving as a key solution to these bottlenecks. In this review, we critically summarize recent advances in separator engineering for addressing the critical challenges facing zinc anodes in ZIBs. Two core strategies for separator optimization in ZIBs have been discussed in detail: (1) modification of commonly used GF separators by incorporating functional materials like MOFs, polymers, biomass, and carbon materials to enhance mechanical strength, ion selectivity, and interfacial compatibility. (2) development of cellulose-based, biomass-based, and Janus-type separators that leverage their inherent structural advantages and functional properties to fundamentally improve ion transport efficiency and electrode stability. These strategies achieve long-term anode stability through precise control of pore structures, surface functional groups, and interfacial interactions, providing essential support for performance enhancement in ZIBs. In addition, we conducted a comparative study on the performance and functional characteristics of GF separators made from different materials and novel separators (Tables 1–3).

A crucial aspect of separator engineering involves balancing manufacturing cost with battery performance. The separator design schemes of ZIBs directly affect energy density by regulating ion transport efficiency, suppressing zinc dendrites and side reactions, and optimizing electrode–electrolyte interface stability: functionalized modified separators leverage ion sieving, catalytic conversion, or oriented deposition induction effects to reduce capacity fading and polarization loss, improve the reversible capacity and cycling stability of batteries, and indirectly raise the upper limit of energy density; in contrast, traditional GF separators, due to uneven pores and insufficient mechanical strength, are prone to causing dendrite penetration and side reactions, thereby limiting the exertion of energy density. In terms of cost, natural biomass-based separators, low-cost mineral coatings, and simple preparation processes (vacuum filtration, solution impregnation) can reduce material and production costs, making them suitable for large-scale applications; while modifiers such as GO and MOFs or complex synthesis processes will increase the preparation cost of separators, but this disadvantage can be partially offset by improving battery cycle life and reducing replacement frequency.

Significant research effort has been directed toward separator engineering to address the key issues of zinc dendrite growth, HER, and anode corrosion in ZIBs. However, due to the complexity of zinc anode reactions, both challenges and opportunities will be present in future research on zinc anodes. First, rational design and fabrication of functional separators with uniformly and vertically aligned nanochannels to guide the directional and uniform flux of Zn^{2+}. These advanced separators with specific sites are expected to reduce nucleation overpotential of Zn^{2+}, guide uniform nucleation, suppress dendrite growth, and inhibit anode corrosion. Second, development of evaluation systems combining in situ interface characterization with performance testing to reveal the evolution mechanisms of zinc anodes during cycling. Due to the integrated properties of separators in ZIBs, conventional ex situ characterization is not sufficient to reflect the real structural changes and effects on zinc anodes. It is essential to combine in situ characterization to achieve real-time monitoring of the zinc deposition evolution, which provides direct evidence on the critical roles of functional separators for improving zinc anodes [73, 148].

Future practical and promising research directions for separators in ZIBs can focus on low-cost and scalable systems. Commercial substrates such as cellulose, nonwoven fabrics, and GF should be prioritized, with simple modification strategies adopted. By introducing polar functional groups, inorganic nanocoatings, or ion-regulating layers, the separators can effectively suppress zinc dendrites, reduce side reactions, and stabilize the electrode–electrolyte interface. Low cost is the core prerequisite for ZIBs to achieve market-oriented applications, focusing on replacing high-priced components with low-cost raw materials, simplifying modification processes, and reducing preparation energy consumption. It can be promoted specifically from two aspects: first, prioritize the selection of low-cost, abundant commercial substrates and modification materials and abandon high-priced rare raw materials. For example, use industrial-grade cellulose, ordinary nonwoven fabrics, and low-cost GF as substrates to replace high-purity special fibers and achieve modification through simple physical mixing, dip-coating, and other methods, which not only reduces raw material costs but also simplifies the modification process. Second, optimize the preparation process to reduce high-energy-consuming and high-cost steps. For instance, replace traditional high-temperature calcination and vacuum coating processes with low-cost processes such as room-temperature dip-coating and roll-coating to reduce equipment investment and production energy consumption. Meanwhile, reducing the loading amount of modifiers by regulating the dispersibility of modifiers and optimizing the interface bonding method will further decrease the raw material cost per unit product.

Large-scale preparation is the key for ZIBs separators to move from laboratory to industrial application. It can be broken through specifically from two aspects: first, develop continuous preparation processes to meet the needs of industrial production lines, such as designing integrated production lines for continuous dip-coating, continuous drying, and roll-to-roll cutting to replace the laboratory batch preparation mode. Second, optimize the stability and repeatability of the preparation process and establish a standardized production parameter system, for example, clarify the optimal range of key parameters such as modifier concentration, coating thickness, drying temperature, and time to solve the bottleneck of poor performance consistency of separators in large-scale production.

Besides, theoretical calculations are effective and facile approaches to simulate Zn^{2+} flux distribution and deposition behavior, which provide theoretical support for function-oriented separator design. In the research on separators for ZIBs, theoretical calculation and characterization techniques such as DFT, MD, and HOMO/LUMO analysis have become core tools for deciphering interfacial mechanisms and optimizing separator performance. DFT calculations reveal the intrinsic interaction mechanisms among modified components through simulations of adsorption energy, charge density distribution, surface energy, and other parameters. For example, Zhu et al. introduced ZSM-5 zeolite into a GF separator to promote the desolvation of Zn^{2+}, enhance its binding with water, and effectively suppress the HER [149]. DFT calculations showed that ZSM-5 exhibits strong adsorption toward VO_2^+ and H_2O, thereby significantly inhibiting vanadium decomposition. MD simulations focus on dynamic processes and intuitively present the migration trajectories of Zn^{2+} in the nanochannels of separators, the wetting kinetics between electrolytes and separators, and the evolution of zinc dendrites during cycling, which helps optimize the pore structure and interfacial compatibility of separators. For instance, Wang et al. modified a GF separator with oxygen-deficient ultrathin zirconium phosphate (D-ZrP) nanosheets to prepare a functional separator (GFZP) with ion-releasing capability [150]. MD simulations confirmed that the GFZP separator can rapidly and directionally release adsorbed anions and cations under a weak electric field. This not only accelerates the fast migration of Zn^{2+} but also replenishes SO_4^{2-} via reverse diffusion, thus alleviating the salt depletion issue at the zinc anode interface, stabilizing the electric field distribution, and inducing dendrite-free zinc deposition.

HOMO/LUMO energy level analysis is mostly used for the screening of organic modifiers or electrolyte additives. Charge transfer efficiency is evaluated via energy level matching to assist in the design of separator systems with high conductivity and low interfacial impedance. For example, Han et al. established a predictive framework that correlates the highest occupied molecular orbital energy level with the adsorption and reduction behavior of Zn^{2+}. Guided by this model, 4-dimethylaminopyridine was identified as a high-performance additive [151]. By achieving kinetic matching between mass transport and deposition processes, this additive slows down interfacial charge transfer, mitigates local ion depletion, and thus inhibits zinc dendrite formation. Furthermore, it can effectively repel interfacial water molecules and significantly suppress side reactions. The combined application of these techniques provides comprehensive support for the structural and functional optimization of separators from microscopic mechanisms to macroscopic performance, accelerating the research and development of high-performance ZIBs [111, 152]. Overall, these approaches will facilitate more precise design of advanced separators via separator engineering for high-stability zinc anodes, thus accelerating the practical applications of ZIBs.

Acknowledgments

Dr. Jian Wang thanks the fellowship support provided by the Alexander von Humboldt Foundation.

Open Access funding enabled and organized by Projekt DEAL.

Funding

The authors thank financial support from thethe National Key R&D Program of China (2021YFA1201503), National Natural Science Foundation of China (No. 22572217, 22279161, 22309144, 52202244, 52436005), Opening funding from Key Laboratory of Engineering Dielectrics and Its Application (Harbin University of Science and Technology) (No. KFM202507, Ministry of Education), Open Project of Inner Mongolia Engineering Research Center of Lithium-Sulfur Battery Energy Storage (No. MDK2025071), and the Research Foundation for Advanced Talents of Jiangsu University, China (No. 22JDG010).

Conflicts of Interest

The authors declare no conflicts of interest.

References

1. Y. Shen, S. Liu, H. Liu, and H. Zhao, "Single-Source Realization of Na-Doped and Carbon-Coated LiMnPO4 Nanocomposite for Enhanced Performance of Li-Ion Batteries," *Journal of Solid State*

Electrochemistry : Current Research and Development in Science and Technology 27 (2023): 1055.

2. Y. Zhang, S. Yang, Y.-J. Zhu, et al., "Synergistically Regulating the Separator Pore Structure and Surface Property toward Dendrite-Free and High-Performance Aqueous Zinc-Ion Batteries," *Journal of Colloid and Interface Science* 656 (2024): 566.

3. J. Wang, J. Zhang, Y. Zhang, et al., "Atom-Level Tandem Catalysis in Lithium Metal Batteries," *Advanced Materials* 36 (2024): e2402792.

4. D. Lu, R. Li, L. Lv, et al., "Ligand-Channel-Enabled Ultrafast Li-Ion Conduction," *Angewandte Chemie International Edition* 65 (2025): e18546.

5. Y. Wei, M. Wang, M. Zhang, T. Cai, Y. Huang, and M. Xu, "Advancements, Challenges, and Future Trajectories in Advanced Battery Safety Detection," *Electrochemical Energy Reviews* 8 (2025): 10.

6. J. Wang, J. Zhang, J. Wu, et al., "Interfacial "Single-Atom-in-Defects" Catalysts Accelerating Li^{+} Desolvation Kinetics for Long-Lifespan Lithium-Metal Batteries," *Advanced Materials* 35 (2023): e2302828.

7. B. X. Chen, X. M. Cheng, H. F. Yang, et al., "Reviews of High-Longevity Aqueous Zinc Metal Batteries Achieved by Programmable Interface Architectures," *Energy & Environmental Materials* 9 (2025): e70176.

8. J. Zhang, C. You, H. Lin, and J. Wang, "Electrochemical Kinetic Modulators in Lithium–Sulfur Batteries: From Defect-Rich Catalysts to Single Atomic Catalysts," *Energy & Environmental Materials* 5 (2022): 731.

9. Q. H. Guan, J. Wang, Q. Zhuang, et al., "Self-Tandem Catalysis of Fast Mg^{2+} Desolvation and Sulfur Conversions for Ultrahigh-Performance Mg–S Batteries *via* Serially-Assembled Atomic Reactors," *Energy & Environmental Science* 17 (2024): 3765.

10. J. Wang, L. Jia, J. Zhong, et al., "Single-Atom Catalyst Boosts Electrochemical Conversion Reactions in Batteries," *Energy Storage Materials* 18 (2019): 246.

11. L. J. Jia, H. F. Hu, X. M. Cheng, et al., "Toward Low-Temperature Zinc-Ion Batteries: Strategy, Progress, and Prospect in Vanadium-Based Cathodes," *Advanced Energy Materials* 14 (2024): 2304010.

12. Z. Wu, Y. Zuo, Y. Zhang, et al., "Modulating Inner Helmholtz Layer by Electrocatalytically Sieving [Zn(H2O)6]2+ for 10000-Cycle Zinc-Ion Hybrid Capacitors under Extremely Harsh Conditions," *Energy Storage Materials* 70 (2024): 103463.

13. L. Zheng, H. Li, M. Gao, et al., "Screening Ammonium-Based Cationic Additives to Regulate Interfacial Chemistry for Aqueous Ultra-Stable Zn Metal Anode," *Advanced Science* (2024): e2407102.

14. W. Wang, J. Dong, H. Hu, et al., "Gradient Desolvation–Diffusion Kinetic Layer Promoters for Low-Temperature Dendrite-Free Zn Metal Batteries," *Nano Letters* 25 (2025): 10376.

15. X. Yu, S. Yuan, L. Yan, et al., "Relay Storage of Protons and Zinc Ions Enables Practical High-Mass-Loading Organic Electrodes," *Angewandte Chemie International Edition in English* (2026): e8137922, early view https://doi.org/10.1002/anie.8137922.

16. S. Zhang, Q. Gou, W. Chen, et al., "Co-Regulating Solvation Structure and Hydrogen Bond Network via Bio-Inspired Additive for Highly Reversible Zinc Anode," *Advanced Science* 11 (2024): 2404968.

17. X. Zhang, Q. Tang, H. Luo, et al., "Hydrogen Bond Reconstruction Maneuver in Eutectic Electrolyte Enables Ultralong-Lifespan Zinc-Ion Batteries," *Journal of the American Chemical Society* 147 (2025): 39440.

18. J. Zhang, R. He, L. Jia, et al., "Strategies for Realizing Rechargeable High Volumetric Energy Density Conversion-Based Aluminum–Sulfur Batteries," *Advanced Functional Materials* 33 (2023): 2305674.

19. J. Zhang, L. Pan, L. Jia, et al., "Delocalized Electron Engineering of MXene-Immobilized Atomic Catalysts toward Fast Desolvation and Dendritic Inhibition for Low-Temperature Zn Metal Batteries," *Nano Letters* 25 (2025): 3756.

20. Y. Zhang, H. Zhou, J. Gu, et al., "Homogeneous Low-Tortuosity Membrane with Fast Ion Transfer towards Life-Durable Low-Temperature Zinc Metal Batteries," *Energy Storage Materials* 76 (2025): 104161.

21. W. Wang, C. Li, W. Zhuang, et al., "Rational Constructions of High-Performance Flexible Aqueous Gel-State Zinc Ionic Batteries," *Advanced Functional Materials* 35 (2025): 2423311.

22. J. Zhang, C. Han, L. Pan, et al., "Low-Temperature Dendrite-Free Zn Metal Battery Catalyzed by TiN-Enhanced Diffusion Layer," *Journal of Power Sources* 640 (2025): 236810.

23. J. Dong, X. Cheng, H. Yang, et al., "Suspension Electrolytes with Catalytically Self-Expediating Desolvation Kinetics for Low-Temperature Zinc Metal Batteries," *Advanced Materials* (2025): e2501079.

24. H. Du, Z. Yi, H. Li, et al., "Separator Design Strategies to Advance Rechargeable Aqueous Zinc Ion Batteries," *Chemistry – A European Journal* 30 (2024): e202303461.

25. C. Yan, L. Zhu, P. Li, et al., "Multi-level Zn^{2+}-Buffering Interphase Enabled by Hierarchical Nanostructure Engineering of Gel Polymers for Highly Reversible Zinc Metal Anode," *Advanced Materials* 38 (2025): e15316.

26. X. Xu, Y. Chen, D. Zheng, et al., "Ultra-Fast and Scalable Saline Immersion Strategy Enabling Uniform Zn Nucleation and Deposition for High-Performance Zn-Ion Batteries," *Small* 17 (2021): 2101901.

27. X. Cheng, Y. Zuo, Y. Zhang, et al., "Superfast Zincophilic Ion Conductor Enables Rapid Interfacial Desolvation Kinetics for Low-Temperature Zinc Metal Batteries," *Advanced Science* 11 (2024): e2401629.

28. J. Wang, H. F. Hu, L. J. Jia, et al., "Fast Interfacial Electrocatalytic Desolvation Enabling l ow-temperature and l ong-cycle-life Aqueous Zn Batteries," *Infomat* 6 (2024): e12558.

29. Z. Fang, J. Li, L. Xiang, et al., "Kinetic Regulation of Zn(002) Textured Interfaces for Highly Reversible Zn–iodine Batteries," *Energy Storage Materials* 82 (2025): 104592.

30. J. Heo, D. Dong, Z. Wang, F. Chen, and C. Wang, "Electrolyte Design for Aqueous Zn Batteries," *Joule* 9 (2025): 101844.

31. Z. Liu, Y. Zhang, M. Li, et al., "Lean-Water Gel Electrolyte Enables Zinc Ion Battery at −70°C," *Angewandte Chemie International Edition* 64 (2025): e202511520.

32. Z. Yang, Q. Zhang, T. Wu, et al., "Thermally Healable Electrolyte-Electrode Interface for Sustainable Quasi-Solid Zinc-ion Batteries," *Angewandte Chemie International Edition* 63 (2024): e202317457.

33. Z. Guo, Z. Liu, Y. Zhang, et al., "Ultrastrong Bioinspired "brick-and-Mortar" Artificial SEI for Dendrite-Free Zn Anode," *Matter* 8 (2025): 102269.

34. C. Zhao, Z. Liu, Y. Zhang, et al., "Tolerant Molecular Engineering for High-Rate and Ultra-Long Cycle Life Zinc Anode," *Advanced Science* 12 (2025): e08628.

35. X. Fang, C. Hu, X. Sun, H. Wang, and J. Li, "Robust Hybrid Solid Electrolyte Interface Induced by Zn-Poor Electric Double Layer for A Highly Reversible Zinc Anode," *Advanced Energy Materials* 14 (2023): 2302499.

36. Z. Liu, G. Xu, Y. Zhang, et al., "Unveiling Zinc Stripping and Molecular Engineering for High-Performance Zinc Anode," *Angewandte Chemie International Edition* 64 (2025): e202501960.

37. M. Yang, J. Zhu, J. Lin, et al., "A Guest Cation Screening Principle for Enabling Customized Cathode/Electrolyte Interface Chemistry and Self-Enhanced Aqueous Zinc-Ion Batteries," *Angewandte Chemie International Edition* 64 (2025): e202510893.

38. C. F. J. Francis, I. L. Kyratzis, and A. S. Best, "Lithium-Ion Battery Separators for Ionic-Liquid Electrolytes: A Review," *Advanced Materials* 32 (2020): 1904205.

39. H. Ying, S. Liu, Q. Zhao, et al., "Functionalized Separator with Integrated Mass Transfer Selectivity and Kinetics Regulation toward Durable Zn Anodes," *ACS Nano* 19 (2025): 40484.

40. Y. Sun, Q. Jian, T. Wang, et al., "A Janus Separator towards Dendrite-Free and Stable Zinc Anodes for Long-Duration Aqueous Zinc Ion Batteries," *Journal of Energy Chemistry* 81 (2023): 583.

41. J. Zhu, M. Yanilmaz, K. Fu, et al., "Understanding Glass Fiber Membrane Used as a Novel Separator for Lithium–sulfur Batteries," *Journal of Membrane Science* 504 (2016): 89.

42. Y. Liu, J.-X. Liu, W. Deng, H.-F. Li, G.-X. Yu, and J. Xiang, "Uniform Zinc Deposition on Carbon Dot Modified Graphite Felt Electrode with Enhanced Electrochemical Performance for Alkaline Zinc-Based Flow Batteries," *Journal of Power Sources* 632 (2025): 236366.

43. W. Liu, S. Zhao, J. Lin, Y. Yang, Y. Chen, and G. Zeng, "Recent Advances in Cellulose-Based Separators for Zinc Ion Batteries: A Review," *International Journal of Biological Macromolecules* 306 (2025): 141326.

44. H. Li, S. Askari, A. Kulachenko, M. Ek, and O. Sevastyanova, "Eco-Friendly and Strong Lignin-Containing Microfibrillated Cellulose Films for High-Performance Separators of Aqueous Zinc Batteries," *International Journal of Biological Macromolecules* 290 (2025): 138711.

45. Y. Zhang, X. Li, L. Fan, Y. Shuai, and N. Zhang, "Ultrathin and Super-Tough Membrane for Anti-Dendrite Separator in Aqueous Zinc-Ion Batteries," *Cell Reports. Physical Science* 3 (2022): 100824.

46. W. Yang, J. Zeng, A. Lang, K. Zhou, W. Yang, and X. Peng, "Biomass-Based Separators for Aqueous Zinc-Ion Batteries: Advantages, Strategies, and Perspectives," *Journal of Materials Chemistry A* 13 (2025): 31978.

47. B. Li, Y. Zeng, W. Zhang, et al., "Separator Designs for Aqueous Zinc-Ion Batteries," *Science Bulletin* 69 (2024): 688.

48. Y. Zong, H. He, Y. Wang, et al., "Functionalized Separator Strategies toward Advanced Aqueous Zinc-Ion Batteries," *Advanced Energy Materials* 13 (2023): 2300403.

49. L. Li, S. Jia, Z. Cheng, and C. Zhang, "Improved Strategies for Separators in Zinc-Ion Batteries," *ChemSusChem* 16 (2023): 202202330.

50. S. Ponnada, M. S. Kiai, R. Krishnapriya, R. Singhal, and R. K. Sharma, "Lithium-Free Batteries: Needs and Challenges," *Energy & Fuels : an American Chemical Society Journal* 36 (2022): 6013.

51. W. Lu, C. Zhang, H. Zhang, and X. Li, "Anode for Zinc-Based Batteries: Challenges, Strategies, and Prospects," *Acs Energy Letters* 6 (2021): 2765.

52. T. N. T. Tran, S. Jin, M. Cuisinier, B. D. Adams, and D. G. Ivey, "Reaction Mechanisms for Electrolytic Manganese Dioxide in Rechargeable Aqueous Zinc-Ion Batteries," *Scientific Reports* 11 (2021): 20777.

53. B. Liu, Z. Xu, C. Wei, et al., "Re-Understanding and Mitigating Hydrogen Release Chemistry toward Reversible Aqueous Zinc Metal Batteries," *EScience* 5 (2025): 100330.

54. L. Wang, J. Guan, N. Li, et al., "Amine-Functionalized MIL-125 Separator and MOF-Derived Carbon Host for High-Performance Aqueous Zinc-Iodine Batteries," *Advanced Energy Materials* 15 (2025): e04201.

55. Y. Wu, M. Xie, K. Fu, et al., "Realizing Lean-Electrolyte Zinc-Ion Batteries via An Ultrathin and Cost-Effective Separator," *Advanced Functional Materials* (2025): e27567, early view https://doi.org/10.1002/adfm.202527567.

56. F. Zhu, J. Wang, Y. Zhang, et al., "Low-Temperature Lithium Metal Batteries Achieved by Synergistically Enhanced Screening Li^+ Desolvation Kinetics," *Advanced Materials* 37 (2025): e2411601.

57. J. Zhang, F. Liu, R. He, et al., "Taming Interfacial Ion-Dipole Interactions With d-Orbital Delocalized Electron Catalysis Expediates Low-Temperature Li Metal Batteries," *Advanced Materials* 37 (2025): e10894.

58. J. Wang, L. Li, H. Hu, et al., "Toward Dendrite-Free Metallic Lithium Anodes: From Structural Design to Optimal Electrochemical Diffusion Kinetics," *ACS Nano* 16 (2022): 17729–17760.

59. J. Wang, J. Zhang, S. Duan, et al., "Lithium Atom Surface Diffusion and Delocalized Deposition Propelled by Atomic Metal Catalyst toward Ultrahigh-Capacity Dendrite-Free Lithium Anode," *Nano Letters* 22 (2022): 8008.

60. J. Zhang, L. Li, M. Yang, et al., "Electron-Delocalization Catalyzers for High Performance, Low-Temperature Li–S Batteries," *Chemical Communications* 60 (2024): 13891.

61. H. Yang, J. Wang, P. Zhang, et al., "Dielectric-Ion-Conductive ZnNb2O6 Layer Enabling Rapid Desolvation and Diffusion for Dendrite-Free Zn Metal Batteries," *Journal of Energy Chemistry* 100 (2025): 693.

62. M. Zhang, W. Xu, X. Han, et al., "Unveiling the Mechanism of the Dendrite Nucleation and Growth in Aqueous Zinc Ion Batteries," *Advanced Energy Materials* 14 (2023): 2303737.

63. H. H. Li, F. L. Wu, J. Wang, et al., "Anode-Free Sodium Metal Batteries: Optimisation of Electrolytes and Interphases," *Energy & Environmental Science* 18 (2025): 3887-3916.

64. Z. Zhang, J. Wang, H. Qin, et al., "Constructing an Anion-Braking Separator to Regulate Local Li^+ Solvation Structure for Stabilizing Lithium Metal Batteries," *ACS Nano* 18 (2024): 2250.

65. X. Li, H. Yu, D. A. Alshammari, et al., "Regulation of Proton Vehicle Migration for Synergetic Interfacial Stability Enables Long-Lasting Ah-Level Zinc-Ion Batteries," *Advanced Materials* 38 (2025): e16427.

66. H. Li, J. Wang, J. Zhang, et al., "Prospects of Single Atom Catalysts for Dendrite-Free Alkali Metal Batteries," *Green Chemistry* 26 (2024): 10366.

67. H. F. Yang, F. Q. Liu, B. X. Chen, et al., "Edge-Electron Induced Ferrimagnetic Effect to Accelerate Interfacial Desolvation Kinetics toward Dendrite-Free Zn Metal Batteries," *Chemical Engineering Journal* 519 (2025): 164989.

68. Q. Guan, Q. Zhuang, W. Xu, et al., "Accelerated Kinetics of Desolvation and Redox Transformation Enabled by MOF Sieving for High-Loading Mg-S Battery," *Advanced Functional Materials* (2025): 2506397.

69. C. Zhou, L. Shan, Z. Xing, et al., "Interface Layer Engineering of Zinc Anode for Durable Seawater-Based Zinc-Ion Batteries," *Advanced Materials* 38 (2025): e16045.

70. P. Chen, T. Wang, D. He, et al., "Delocalized Isoelectronic Heterostructured $FeCoO_x S_y$ Catalysts with Tunable Electron Density for Accelerated Sulfur Redox Kinetics in Li-S Batteries," *Angewandte Chemie International Edition in English* 62 (2023): e202311693.

71. X. Zhang, X. Y. Li, Y. Z. Zhang, et al., "Accelerated Li^+ Desolvation for Diffusion Booster Enabling Low-Temperature Sulfur Redox Kinetics via Electrocatalytic Carbon-Grazfted-CoP Porous Nanosheets," *Advanced Functional Materials* 33 (2023): 2302624.

72. Y. Xue, W. Li, R. Liu, et al., "Functionalized Separator Strategies Accelerate the Development of Zinc-Ion Batteries," *IScience* 28 (2025): 112787.

73. Y. He, D. Xiong, M. Chen, et al., "Modulating Ion-Dipole and Dipole–Dipole Interactions for Stable Wide-Temperature-Range Lithium–Sulfur Batteries Enabled by Quantum-Dot Catalysts," *Angewandte Chemie International Edition in English* 64 (2025): e202512168.

74. Y. Tan, D. Chen, T. Yao, et al., "Tailoring Zn^{2+} Flux by an Ion Acceleration Layer Modified Separator for High-Rate Long-Lasting Zn Metal Anodes," *Advanced Science* 11 (2024): 2407410.

75. D. Duan, W. Zhao, K. Chen, et al., "MOF-71 Derived Layered Co-CoP/C for Advanced Li-S Batteries," *Journal of Alloys and Compounds* 886 (2021): 161203.

76. A. E. Baumann, R. I. Anayah, and V. S. Thoi, "Phosphorus-Functionalized Organic Linkers Promote Polysulfide Retention in MOF-Based Li–S Batteries," *Acs Applied Energy Materials* 5 (2022): 15302.

77. F. Na, X. Li, J. Wang, et al., "Immobilizing Single Atom on High-Entropy Oxides as Separator Regulators for Catalyzing Low-Temperature Lithium-Sulfur Battery," *Energy Storage Materials* 78 (2025): 104228.

78. L. Yuan, J. Xu, Z. Yang, Q. Su, and J. Li, "Zinc Oxide Anode Modified with Zeolite Imidazole Structure Achieve Stable Circulation for Zinc–nickel Secondary Battery," *Journal of Power Sources* 517 (2022): 230696.

79. Z. Ou, X. Li, Y. Wang, D. He, W. Gan, and Q. Yuan, "Ionic Sieve 2D-MOF Modified Anode for Long Durable Aqueous Zinc Ion Battery with High Capacity," *Electrochimica Acta* 523 (2025): 145987.

80. W. Zhang, X. Zhu, L. Kang, et al., "Stabilizing Zinc Anode Using Zeolite Imidazole Framework Functionalized Separator for Durable Aqueous Zinc-ion Batteries," *Journal of Energy Chemistry* 90 (2024): 23.

81. H. Di, Y. An, J. Yang, D. Luan, and X. W. Lou, "Fluorine Modified Zeolitic Imidazolate Framework Enables Long-Life Zn–I_2 Batteries by Suppression of Polyiodide Shuttle," *Angewandte Chemie International Edition* 64 (2025): e202513312.

82. X. Li, Z. Yan, J. Zhang, et al., "Synergistic Engineering of Structural and Electronic Regulation in Necklace-Like UiO-66/ACNT Structure toward Lithium-Sulfur Batteries with Fast Polysulfide Redox," *Chemical Engineering Journal* 493 (2024): 152554.

83. B. Li, J. Liu, Z. Nie, et al., "Metal–Organic Frameworks as Highly Active Electrocatalysts for High-Energy Density, Aqueous Zinc-Polyiodide Redox Flow Batteries," *Nano Letters* 16 (2016): 4335.

84. Y. Song, P. Ruan, C. Mao, et al., "Metal–Organic Frameworks Functionalized Separators for Robust Aqueous Zinc-Ion Batteries," *Nano-Micro Letters* 14 (2022): 218.

85. R. Chen, G. Zhang, H. Zhou, et al., "Robust Zinc Anode Enabled by Sulfonate-Rich MOF-Modified Separator," *Small* 20 (2023): 2305687.

86. S. Nan, W. Wei, X. Su, et al., "Imidazole-Rich Polymer Modified Glass Fiber Separators with Low Electrolyte Uptake for Dendrite-Free and Corrosion-Free Zinc Metal Batteries," *Chemical Engineering Journal* 504 (2025): 158634.

87. J. Wang, H. Hu, J. Zhang, et al., "Hydrophobic Lithium Diffusion-Accelerating Layers Enables Long-Life Moisture-Resistant Metallic Lithium Anodes in Practical Harsh Environments," *Energy Storage Materials* 52 (2022): 210.

88. J. Wang, H. Hu, S. Duan, et al., "Construction of Moisture-Stable Lithium Diffusion-Controlling Layer toward High Performance Dendrite-Free Lithium Anode," *Advanced Functional Materials* 32 (2021): 2110468.

89. J. Wang, J. Yang, Q. Xiao, et al., "In Situ Self-Assembly of Ordered Organic/Inorganic Dual-Layered Interphase for Achieving Long-Life Dendrite-Free Li Metal Anodes in LiFSI-Based Electrolyte," *Advanced Functional Materials* 31 (2020): 2007434.

90. Y. Liu, S. Liu, X. Xie, et al., "A Functionalized Separator Enables Dendrite-free Zn Anode via Metal-polydopamine Coordination Chemistry," *InfoMat* 5 (2022): e12374.

91. F. Ilyas, W. Li, A. Iqbal, et al., "Highly Reversible Zinc Anode Enabled by Composite Tailored Polyimide Separator," *Nano Energy* 128 (2024): 109807.

92. S. Liu, L. Fang, R. He, et al., "Highly Stable Zinc Anodes Achieved by Regulating Zinc Ions Deposition through Polyimide Glue Functionalized Composite Separators," *Journal of Power Sources* 614 (2024): 235002.

93. R.-h. Li, B.-b. Sui, P.-f. Wang, et al., "Modulation of Zinc Deposition Behaviour by Electrostatically Spun PAN-ZnTFSI Fibre Layer on Separator for Aqueous Zinc Ion Batteries," *Journal of Alloys and Compounds* 997 (2024): 174899.

94. Y. Fang, X. Xie, B. Zhang, et al., "Regulating Zinc Deposition Behaviors by the Conditioner of PAN Separator for Zinc-Ion Batteries," *Advanced Functional Materials* 32 (2021): 2109671.

95. B. Wu, P. Wang, H. Yang, et al., "Design on Modified Glass Fiber Separator by Graphite Fluoride Nanoflakes for Zn Metal Anodes with Highly Reversibility," *Journal of Power Sources* 580 (2023): 233323.

96. F. Shen, H. Du, H. Qin, et al., "Mediating Triple Ions Migration Behavior via a Fluorinated Separator Interface toward Highly Reversible Aqueous Zn Batteries," *Small* 20 (2023): 2305119.

97. A. Feng, X. Zhu, Y. Chen, et al., "Functional Biomass-Derived Materials for the Development of Sustainable Batteries," *ChemElectroChem* 11 (2024): e202400086.

98. Q. Wu, J. Huang, J. Zhang, et al., "Multifunctional Cellulose Nanocrystals Electrolyte Additive Enable Ultrahigh-Rate and Dendrite-Free Zn Anodes for Rechargeable Aqueous Zinc Batteries," *Angewandte Chemie International Edition* 63 (2024): e202319051.

99. D.-H. Wu, H. Huang, M. Ul Haq, L. Zhang, J.-J. Feng, and A.-J. Wang, "Lignin-Derived Iron Carbide/Mn, N, S-Codoped Carbon Nanotubes as a High-Efficiency Catalyst for Synergistically Enhanced Oxygen Reduction Reaction and Rechargeable Zinc-Air Battery," *Journal of Colloid and Interface Science* 647 (2023): 1.

100. Y. Liu, L. Zhou, S. Liu, et al., "Fe, N-Inducing Interfacial Electron Redistribution in NiCo Spinel on Biomass-Derived Carbon for Bi-functional Oxygen Conversion," *Angewandte Chemie International Edition* 63 (2024): e202319983.

101. H.-W. Liang, Z.-Y. Wu, L.-F. Chen, C. Li, and S.-H. Yu, "Bacterial Cellulose Derived Nitrogen-Doped Carbon Nanofiber Aerogel: An Efficient Metal-Free Oxygen Reduction Electrocatalyst for Zinc-Air Battery," *Nano Energy* 11 (2015): 366.

102. J. Guo, Y. Wang, S. Li, et al., "Regulating Zinc Deposition for Dendrite-Free Aqueous Zinc-Ion Batteries: A Zincophilic Chitosan Polyelectrolyte Hydrogel Modified Glass Fiber Separator," *Journal of Alloys and Compounds* 967 (2023): 171708.

103. Q. Gou, H. Luo, L. Qu, et al., "A Seaweed-Inspired Separator for High Performance Zn Metal Batteries: Boosting Kinetics and Confining Side-Reactions," *Journal of Energy Chemistry* 101 (2025): 191.

104. T. Huang, S. Wang, J. Wu, et al., "Triazine and Hydroxyl Covalent Organic Framework Modified Separator for Zn-Ion Fast and Selective Transport and Dendrite-Free Deposition in Zinc–iodine Battery," *Journal of Power Sources* 608 (2024): 234658.

105. S. Chen, L. Tian, X. Feng, H. Bao, and H. Wang, "Biomaterial-Derived Porous Carbon Doped with Heteroatoms as a Separator Coating for High-Energy–density Zn-I Batteries," *Biochar* 6 (2024): 99.

106. S. K. Tiwari, S. Sahoo, N. Wang, and A. Huczko, "Graphene Research and their Outputs: Status and Prospect," *Journal of Science: Advanced Materials and Devices* 5 (2020): 10.

107. J. Wang, X. Jin, C. Li, W. Wang, H. Wu, and S. Guo, "Graphene and Graphene Derivatives Toughening Polymers: Toward High Toughness and Strength," *Chemical Engineering Journal* 370 (2019): 831.

108. W. Yu, L. Sisi, Y. Haiyan, and L. Jie, "Progress in the Functional Modification of Graphene/Graphene Oxide: A Review," *RSC Advances* 10 (2020): 15328.

109. J. Wang, S. Cheng, W. Li, et al., "Robust Electrical "highway" Network for High Mass Loading Sulfur Cathode," *Nano Energy* 40 (2017): 390.

110. J. Wang, L. Jia, H. Lin, and Y. Zhang, "Single-Atomic Catalysts Embedded on Nanocarbon Supports for High Energy Density Lithium–Sulfur Batteries," *ChemSusChem* 13 (2020): 3404.

111. J. Wang, J. Zhang, X. Cheng, et al., "Electrode/Electrolyte Interface Studies of Rechargeable Li Batteries with Interface-Specific Sum Frequency Generation Spectroscopy," *Journal of the American Chemical Society* 147 (2025): 44633.

112. Y. Zhang, X. Xia, B. Liu, et al., "Multiscale Graphene-Based Materials for Applications in Sodium Ion Batteries," *Advanced Energy Materials* 9 (2019): 1803342.

113. C. Xu, R.-s. Yuan, and X. Wang, "Selective Reduction of Graphene Oxide," *New Carbon Materials* 29 (2014): 61.

114. L. Ren, J. Liu, Y. Zhao, et al., "Regulating Electronic Structure of Fe–N_4 Single Atomic Catalyst via Neighboring Sulfur Doping for High Performance Lithium–Sulfur Batteries," *Advanced Functional Materials* 33 (2023): 2210509.

115. Y. Chen, C. Gao, J. Li, et al., "Organic/Inorganic Functional Janus Separator for High-Performance Zinc Anode," *Journal of Energy Storage* 103 (2024): 114442.

116. L. Deng, K. Sun, J. Liu, Z. Li, J. Cao, and S. Liao, "High Performance Aqueous Zinc-Ion Batteries Developed by PANI Intercalation Strategy and Separator Engineering," *Molecules* 29 (2024): 3147.

117. H. Liu, Z. Xin, B. Cao, et al., "Polyhydroxylated Organic Molecular Additives for Durable Aqueous Zinc Battery," *Advanced Functional Materials* 34 (2023): 2309840.

118. H. Wang, W. Zhang, J. Xu, and Z. Guo, "Advances in Polar Materials for Lithium–Sulfur Batteries," *Advanced Functional Materials* 28 (2018): 1707520.

119. S. Lv, M. Su, Z. Li, et al., "Hydrophilic-Zincophobic Separator Enabling by Crystal Structure Regulation toward Stabilized Zn Metal Anode," *Advanced Functional Materials* 34 (2024): 2315910.

120. L. Zhu, X. Guan, Z. Zhang, et al., "Polar-Nonpolar Synergy Toward High-Performance Aqueous Zinc–Iodine Batteries," *Small* 21 (2025): 2500223.

121. S. Liu, Q. Han, C. He, et al., "Ion-Sieving Separator Functionalized by Natural Mineral Coating toward Ultrastable Zn Metal Anodes," *ACS Nano* 18 (2024): 25880.

122. R. Li, T. Xiang, P. Wang, et al., "Regulation of the Anode Electrodeposition Behavior of Aqueous ZincIon Batteries by an l - Alanine - Modified Glass Fiber Separator," *Industrial & Engineering Chemistry Research* 63 (2024): 16164.

123. S.J. Lee, J.H. Choi, I. Hwang, et al., "Interfacial Engineering with BN@cellulose Separator to Suppress Dendrite Growth and Side Reactions in Aqueous Zinc-Ion Batteries," *Electrochemistry Communications* 172 (2025): 107882.

124. W. Zhou, M. Chen, Q. Tian, J. Chen, X. Xu, and C.-P. Wong, "Cotton-Derived Cellulose Film as a Dendrite-Inhibiting Separator to Stabilize the Zinc Metal Anode of Aqueous Zinc Ion Batteries," *Energy Storage Materials* 44 (2022): 57.

125. X. Li, J. Li, Q. Yang, et al., "Homogenizing Zn^{2+} Transport and Deposition by Molecular Aggregation State Regulation of Cellulose Separator for High-Performance Aqueous Zn-Ion Batteries," *Advanced Functional Materials* 36 (2025): e19947.

126. W. Yang, W. Yang, Y. Huang, et al., "Stable Zn Anodes Enabled by All-Cellulose Separators with Synergistic Hydroxyl and Carboxyl Chemistry," *Energy Storage Materials* 80 (2025): 104436.

127. S. Xu, Z. Sun, D. Wei, et al., "Polypyrrole Functionalized Cellulose/Polypropylene Composite Membrane with Zinc Inducing and Dendrite Resistance for Robust Zinc-Ion Batteries," *Journal of Membrane Science* 712 (2024): 123230.

128. P. Li, H. Lv, Z. Li, et al., "The Electrostatic Attraction and Catalytic Effect Enabled by Ionic–Covalent Organic Nanosheets on MXene for Separator Modification of Lithium–Sulfur Batteries," *Advanced Materials* 33 (2021): 2007803.

129. X. Zhu, Z. Xu, T. Zhang, et al., "Ultra-Stable Zinc Anodes Facilitated by Hydrophilic Polypropylene Separators with Large Scale Production Capacity," *Advanced Functional Materials* 34 (2024): 2407262.

130. K. Yu, Y. Wen, M. Yan, et al., "Separator Pore Size Induced Oriented Zn Deposition," *Materials Today Energy* 40 (2024): 101488.

131. R. Xue, Z. Wang, N. Yao, et al., "Multiscale Interfacial Regulation of Zn-V_2O_5 Pouch Cell via Ultrathin Molecular-Engineered Separator," *Advanced Functional Materials* 34 (2024): 2400959.

132. L. Solhi, V. Guccini, K. Heise, et al., "Understanding Nanocellulose–Water Interactions: Turning a Detriment into an Asset," *Chemical Reviews* 123 (2023): 1925.

133. X. Yang, X. Nie, C. Tang, et al., "Biomass Materials for Zinc-Based Sustainable and Green Energy Storage Devices: Strategy and Mechanism," *Nano Research* 18 (2025): 94907031.

134. Q. Wang, J. Zhao, J. Zhang, et al., "Biomass Chitin Nanofiber Separators Proactively Stabilizing Zinc Anodes for Dendrite-Free Aqueous Zinc-Ion Batteries," *Advanced Functional Materials* 34 (2024): 2405957.

135. J. Ma, X. Shi, Z. Wang, et al., "High-Capacity Zinc Anode Enabled by a Recyclable Biomass Bamboo Membrane Separator," *Advanced Materials* 36 (2024): 2406429.

136. Y. Zhang, Z. Liu, X. Li, L. Fan, Y. Shuai, and N. Zhang, "Loosening Zinc Ions from Separator Boosts Stable Zn Plating/Striping Behavior for Aqueous Zinc Ion Batteries," *Advanced Energy Materials* 13 (2023): 2302126.

137. Y. Luo, Y. Yang, Y. Tao, D. Huang, B. Huang, and H. Chen, "Directing the Preferred Crystal Orientation by a Cellulose Acetate/Graphene Oxide Composite Separator for Dendrite-Free Zn-Metal Anodes," *Acs Applied Energy Materials* 4 (2021): 14599.

138. H. Ma, H. Chen, M. Chen, et al., "Biomimetic and Biodegradable Separator with High Modulus and Large Ionic Conductivity Enables Dendrite-Free Zinc-Ion Batteries," *Nature Communications* 16 (2025): 1014.

139. C. Zhang, X. Lan, Q. Liu, L. Yu, Y. Li, and X. Hu, "Bi-Functional Janus All-Nanomat Separators for Acid Scavenging and Manganese Ions Trapping in LiMn2O4 Lithium-Ion Batteries," *Materials Today Physics* 24 (2022): 100676.

140. Y. Li, J. Zhang, C. Zhou, et al., "Flame-Retardant and Thermal-Stable Separator Trapping Polysulfides for Lithium-Sulfur Battery," *Journal of Alloys and Compounds* 826 (2020): 154197.

141. C. Liu, B. Lin, Z. Li, et al., "A Janus Membrane with Asymmetrical Proton Transport for Cross-Communication Harmony for an Extreme Lean Electrolyte Zn–V Battery," *Acs Energy Letters* 10 (2025): 1795.

142. S. Zheng, X. Yang, D. Chen, et al., "A Janus Separator Regulating Zinc Deposition Behavior Synergistically by Cellulose and ZrO_2 Nanoparticles Toward High-Performance Aqueous Zinc-Ion Batteries," *Small* 21 (2024): 2411463.

143. G. Guo, X. Tan, K. Wang, L. Zheng, and H. Zhang, "Regulating Zinc Deposition Behaviors by Functional Cotton Textiles as Separators for Aqueous Zinc-Metal Batteries," *Journal of Power Sources* 553 (2023): 232321.

144. B. Wu, Y. Wu, Z. Lu, et al., "A Cation Selective Separator Induced Cathode Protective Layer and Regulated Zinc Deposition for Zinc Ion Batteries," *Journal of Materials Chemistry A* 9 (2021): 4734.

145. T. Wu, H. Ma, M. Chen, X. Han, Q. Tian, and J. Chen, "Thin and Strong Janus Separator Based on Nanocellulose and Ti3C2Tx for Dendrite-Free Aqueous Zinc-Ion Batteries," *Journal of Energy Storage* 73 (2023): 108851.

146. J. Ju, Y. Zhang, Y. Zhang, et al., *Chemical Engineering Journal* 481 (2024): 148479.

147. Y. Cui, Q. Zhao, X. Wu, et al., "An Interface-Bridged Organic–Inorganic Layer that Suppresses Dendrite Formation and Side Reactions for Ultra-Long-Life Aqueous Zinc Metal Anodes," *Angewandte Chemie International Edition* 59 (2020): 16594.

148. J. Wang, H. Liu, J. Zhang, et al., "Polysulfide-Mediated Solvation Shell Reorganization for Fast Li+ Transfer Probed by in-Situ Sum Frequency Generation Spectroscopy," *Energy Storage Materials* 67 (2024): 103289.

149. D. Wang, L. Chang, Y. Xie, et al., "Zeolite-Filled Glass Fiber Separator Enables Ah-Level Zinc Ion Batteries via Synergistic Dual-Electrodes Regulation," *ACS Nano* 20 (2026): 4279.

150. Y. Chen, G. Zhou, X. Huang, et al., "Alleviating Salt Depletion at the Zinc Anode Interface by an Ion-Releasing Separator to Achieve Ultra-Stable Zinc Anode," *Energy Storage Materials* 78 (2025): 104247.

151. S. Han, Y. Zheng, X. Zhang, et al., "Data-Driven Additive Discovery with HOMO-Descriptor Enables Durable Aqueous Zinc Batteries via Interfacial Kinetics Engineering," *Advanced Materials* 37 (2025): e11814.

152. Y. Wang, K. Liu, H. Xiao, et al., "Delicate Design of Lithium-ion Bridges in Hybrid Solid Electrolyte for Wide-temperature Adaptive Solid-state Lithium Metal Batteries," *InfoMat* 8 (2025): e70095.